The Raymer Manned Mars Airplane:
A Conceptual Design and Feasibility Study

AIAA-2021-1187

Daniel Raymer[1], James French[2], Felix Finger[3], Arturo Gómez[4], Jaspreet Singh[5],
Ramlingam Gyanasampath Pillai[6], Matheus Monjon[7], Joabe Marcos de Souza[8], and Aviv Levy[9]

Conceptual Research Corporation
PO Box 5429, Playa del Rey, CA, USA, 90296-5429, www.aircraftdesign.com

If national governments and certain billionaires have their way, humans will reach Mars sometime in this century and set up permanent bases. Eventually they'll need a way to get around. This paper describes the conceptual design and analysis of a manned[10] Mars airplane configured for exploration, research, cargo transport, photography, and the linking of multiple settlements. Design development is being done by an international team of volunteers based on the configuration concept developed by lead author Dr. Daniel P. Raymer and incorporating rocket propulsion concepts suggested by James French. A two-man vehicle was developed based on overall requirements similar to the capabilities of the classic "Jeep" of WWII fame, namely a crew of two plus cargo to a total of 500 lbs, carried at least 260 nmi. It is assumed that the flight control system will be capable of fully autonomous operation when desired and that when carrying humans, they need not be trained pilots. VTOL operation is assumed due to the deplorable lack of paved runways on Mars. Results to date indicate that, with sufficiently advanced technologies, such a manned Mars airplane should be feasible. The configuration presented herein seems viable ("existence proof") and has certain desirable features but future trade studies may find an even better design.

Aflight over Red Lands
Loved by Nations yet Unborn
See Worlds yet Unmade *…a Martian Haiku by Robert Zubrin*

Nomenclature

AOA	= Angle of Attack
CFD	= Computational Fluid Dynamics
FEA	= Finite Element Analysis
Isp	= Specific Impulse (rocket engines)
L/D	= Lift-to-Drag Ratio
R#	= Reynold's Number
RDS^{win}	= Aircraft design software package *("Raymer's Design System")*
RMMP	= Raymer Manned Mars Plane
VTOL	= Vertical Takeoff and Landing

(For further information and detailed analysis reports see www.aircraftdesign.com/mannedmarsplane.html)

[1] President, Conceptual Research Corporation, AIAA Fellow
[2] JRF Aerospace Consulting, AIAA Fellow
[3] Research Engineer & Ph.D. Candidate, FH Aachen Univ. of Applied Sciences (Germany), AIAA Student Member
[4] Department of Continuum Mechanics and Structural Analysis, University Carlos III of Madrid (Spain)
[5] Lead Designer,Tata Motors Ltd (India), AIAA Member
[6] Graduate Student, University of Texas at Arlington MAE Dpt, AIAA Student Member
[7] Student, Federal University of ABC (Brazil) Dpt of Aerospace Engineering, AIAA Student Member
[8] Graduate Student, University of São Paulo (Brazil) Dpt of Aeronautical Engineering
[9] President, Aviv Innovations (Israel), AIAA Member
[10] Herein "manned" is used in the traditional sense of carrying or being operated from within by one or more human beings of unspecified gender

I. Introduction

Conceptual Research Corporation, with the assistance of an international team of volunteers, is conducting a design feasibility study of a Manned Mars Airplane. This is intended as a utility "jeep" for people who are living on Mars at some time in the future, and is configured for exploration, research, cargo transport, photography, and the linking of various human settlements around the planet. Numerous studies have investigated unmanned Mars airplane designs[1] which are rocketed to Mars and typically unfold during a parachute descent following atmospheric entry. Few if any studies have included a substantial configuration design effort of a manned utility aircraft. This paper is such an attempt.

The air vehicle design concept was developed by lead author Dr. Daniel Raymer for a keynote presentation to the *New Space* online conference sponsored by the AIAA LA-LV Section in April 2020, using rocket propulsion concepts defined by James French. After this presentation, a number of people volunteered to help. Eventually seven of them made substantial contributions covering key disciplines of aerodynamics, structures, stability & control, propulsion, and CAD rendering. This has truly been an international effort with participants in Brazil, Germany, India, Israel, and Spain, facilitated by the internet meeting software we've all used so much in this year of Covid. Their work is described below and contributed significantly to the ongoing evolution of the design.

Being an unfunded effort, the lead author cautions that the conclusions below should be considered with some skepticism. Consider this "food for thought," not the final answer. Also, the volunteers' work was done in parallel and their topics were self-chosen, so there are certain gaps and overlaps. In some cases, their preliminary results are not in agreement due to differing assumptions and methods. A funded study would resolve these differences, advance the concept's believability, and allow us to optimize its design (hint, hint).

II. Operational Concept and Design Requirements

The overall operational concept for the Raymer Manned Mars Plane (RMMP) starts with the assumption of a permanent human presence on Mars[2], with one or more bases on Mars, readily-available electrical energy (solar or nuclear), and large pressurized buildings. Permanent residents of Mars will need a "Jeep-like" mobility capability for getting around and for delivering cargo where needed. The original Jeep, formally the GP503 1⁄4-ton truck, was called by General (later President) Eisenhower "one of three decisive weapons the U.S. had during WWII[3]." It was nominally designed to a 500 lb [227 kg] capability and with enough fuel for 300 miles of range [260 nmi=482 km]. It was designed to be both adaptable and maintainable. Its off-road capabilities are legendary, but top speed was not an important design criterion.

The Raymer Manned Mars Plane is similarly required to carry a two-man crew, with a total of 500 lb [227 kg] capability, and at least 260 nmi [482 km] of range. No speed requirement is set. "Off road" operation is assumed, namely unprepared site operation and vertical takeoff and landing. Substantial ground clearance is required, and the lowest part of the vehicle should fit into the footprint area of a typical small helicopter. Concerns about blowing dust and rocks will impact placement of vertical thrust rockets.

The RMMP is to be optionally manned, capable of carrying two people who need not be pilots. Normally the vehicle would fly itself to a programmed destination carrying cargo or disinterested passengers. When desired, the crew could "take the stick" and fly it using a simplified video game or touchpad controller, and by entering commands such as take off, cruise (direction or destination), climb, descend, turn, altitude hold, or land at a designated spot.

The cabin is sized to a two-man crew and requires a good field of view, to choose safe landing sites and allow excellent photography. An optically-clean forward windshield is desired, hemispherical if possible. Seats must readily fold out of the way for cargo loading when operated in UAV mode, and a large door must be provided to allow loading of cargo. Cabin pressurization is desired for crew comfort and the protection of cargo including food resupply.

While other propulsion modes are certainly feasible for flight on Mars, it was assumed for this study that electric motors with propellers would be used for wing-borne forward flight, and vertical rockets would be used for takeoff and landing. Use of horizontally installed rockets to assist in acceleration to forward flight speed may be desirable.

With electricity assumed to be readily available at the Mars base, the flight vehicle's batteries would be charged from a ground source prior to each flight. Enough energy would be stored for a round-trip flight, out and back, and including two takeoff and landing cycles. Wing-mounted solar cells are included in the design requirements. These probably cannot provide enough energy to fly the aircraft continuously but can extend the range and can trickle-charge the batteries while on the ground. For the initial analysis below, a weight estimate for the solar cells was included but no in-flight energy credit was taken.

Specific design requirements for a Mars flight vehicle must consider the overall conditions on Mars versus Earth. As previously described by the lead author, "The air is a lot less dense on Mars. But the gravity is a lot lower. Do the math – it turns out that if you can fly on Earth at about 100,000 feet [~30000 m], then you can fly on Mars. Assuming, of course, that you can get there first, and that you have a motor that can run in an atmosphere with negligible oxygen, bitter cold, and dust storms.[4]"

The Martian atmosphere has a "sea level" density of just 0.000039 slug/ft^3 [0.0201 kg/m^3] versus 0.00238 [1.225] on Earth. To obtain the same lift under otherwise-identical conditions, a lifting surface must be 61 times as large. But the pull of gravity on Mars is only about a third as much (0.379). Multiplying these together yields the conclusion that, all else being the same, a lifting surface on Mars must be "only" 23.13 times as large.

The physical makeup of the Martian atmosphere also impacts air vehicle design. It is over 95% carbon dioxide which, during winter in either hemisphere, sees up to 25% freeze out of the atmosphere as solid CO^2 "dry" ice. The remainder of the atmosphere is about evenly split between argon and nitrogen, plus trace elements. The speed of sound is only 788 fps [240.2 mps] vs. 1116.5 [340.3] on Earth at sea level. This can pose problems for propellers and helicopter rotors, where the tip speeds may approach sonic conditions more easily than on Earth.

At the same time, the low atmospheric density results in a low Reynold's Number for lifting surfaces, propellers, and helicopter rotors. Low R# leads to increased skin friction drag, increased pressure drag due to flow separation, and reduced maximum lift coefficient. One result of this that, contrary to Earth where extreme slow flight is more efficient for vehicles with huge wings, an airplane on Mars should fly faster to reduce the problems of a low R#.

The winds on Mars, while quite impressive in the movies, are not of such concern. With peak velocities of around 52 kts [97 kph] the wind produces a dynamic pressure of about 0.1 psf [0.5 kg/sm]. This is a gentle breeze on Earth. In the worst case, nose-on to the wing at maximum lift angle of attack, the total lift force would only be about half of the Mars weight of the vehicle described below. However, in a detailed analysis the worst-case wind loads should be considered especially for the structural sizing of the wings, tails, and tail booms. As to in-flight gust loads, analysis indicates that they reach no more than 1.7 g's at the worst case of maneuvering speed.

Getting the RMMP to Mars is here considered "someone else's problem"[5] and does not impact the design. Presumably it would be built on Mars with a mixture of items shipped from the Earth and locally-produced components, perhaps 3D printed. Hopefully feedstocks can be created from the available iron, boron, magnesium, and carbon dioxide.

A final consideration is that this design study is not about designing a vehicle based on a particular set of technologies, but rather about determining how much the technologies must improve to make such a design even possible. Rather than the classic "technology availability date" we are looking for "technology availability needs" and will assess later at what date those may become available. As a rough and hopeful guess, we are shooting for 2030.

III. Rocket Propulsion & Propellants

The overall flight mode chosen for this vehicle is battery-electric propellers plus rockets for vertical takeoff and landing. It is obviously undesirable to use rocket propellants that must be shipped from the Earth, so only locally-obtainable propellants are of interest.

Co-author James French has studied this for many years[6] and notes that the use of Martian resources as a rocket propellant has been acknowledged as a useful and viable technology. With mounting evidence of water existing on Mars, the synthesis of methane from the CO2 atmosphere and water has become a favorite scenario because of relatively high Isp, moderate cryogenic storage and the fact that the CH4 manufacturing process also produces oxygen

to burn with the methane. All that said, the methane option demands that the water be accessible in quantity. That is not easy to assume.

Another option exists that avoids this problem, namely use of CO and O2 (carbon monoxide and oxygen). While the performance of this combination is substantially lower than that of CH4 and O2 (260-295 seconds Isp versus ~360 seconds), it has the virtue that the only feedstock required is the Martian atmosphere. The atmosphere can be compressed, decomposed by thermal and electrochemical processes, and liquefied for storage. A substantial ground-based electrical power source would be required, but that is assumed in this study. For best rocket engine performance, a slightly fuel-rich mixture ratio is preferred. Since the extraction process will, by definition, produce the propellants in a stoichiometric ratio, there could be a bit of oxygen left over to use in the life support system.

It is beyond the scope of this study to detail the hardware required to locally produce CO and O2 from the atmospheric CO2, but a literature search will provide current state of the art. Some experts including co-author French are certain that such machinery could even be carried onboard a flight vehicle for "recharging" the propellant tanks while on the ground using wing-mounted solar cells for electrical power, but that was not assumed for this study. Sufficient propellant for two takeoff-landing cycles would be loaded at the main base, and such tankage is provided in the design study below. Note also that a CO-O2 rocket engine returns the CO2 back to the atmosphere from which it was originally taken. This would avoid polluting the Martian environment from the beginning of humanity's presence there.

IV. Baseline RMMP-1 Configuration Development

Initial conceptual design of the Raymer Manned Mars Plane was done by Dr. Raymer in a frantic two-week period just before the AIAA LA-LV sections online "New Space" conference starting 18 April, 2020. Design work was done using Raymer's RDS^{win}-Professional aircraft design software[7]. RDS^{win} is an integrated design environment which includes a design layout module for concept development, with built-in classical analysis modules for aerodynamics, weights, propulsion, stability, cost, performance, range, sizing, and optimization. The methods employed are largely those described in Raymer's textbook *Aircraft Design: A Conceptual Approach*[8].

The resulting CAD geometry was exported in IGES format for rendering in RhinoCAD and later use in CFD and structural design software. The analysis routines of RDS^{win} were used for an assessment of aerodynamics and mass properties, with adjustments for flight conditions on Mars. Those results were used in a spreadsheet analysis based on Raymer's "Simplified Aircraft Design for Homebuilders" spreadsheet[9], suitably modified for conditions on Mars and the use of electric power for propulsion.

The initial design work began with the cabin, sized for two people in an upright seated position with space behind for cargo. To minimize the weight penalty of pressurization, the cabin geometry deliberately resembles an autoclave having a circular cross section, an integral isotensoid aft pressure bulkhead, and a transparent hemisphere as the front bulkhead. Like the door of an autoclave, it would have latches around the circumference and would pivot sideways to open. Small side windows are also provided.

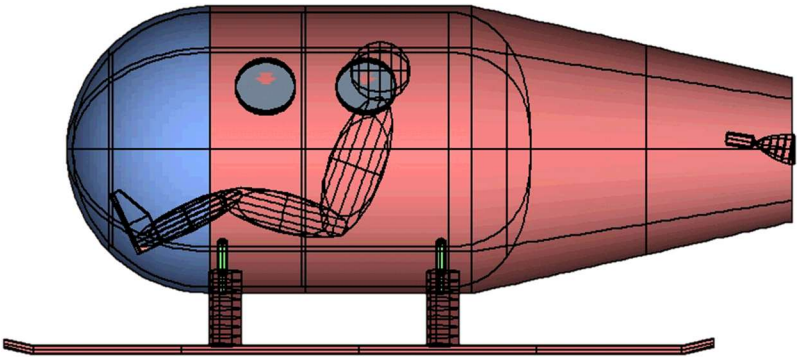

Figure 1 RMMP Cabin

The fuselage aft of the pressure vessel is simply tapered to a flat final bulkhead on which two rocket engines are affixed, if needed. A later trade study should look at the potential drag savings of this versus a more-aerodynamic but more difficult to fabricate shaping. Helicopter-like landing skids were used, with highly-damped shock absorbers to reduce bounce tendencies. They are low to the ground so that people and cargo can readily be loaded.

The wing layout started with a spreadsheet trade study of the wing loading required for flight versus the cruising speed. Flight on Mars will obviously require a huge wing, which on Earth is usually associated with a slow flight speed. On Mars though, a higher speed will allow a smaller wing (still huge) and also helps to avoid an excessively low Reynold's Number. Another issue driving wing loading is the stall speed. With takeoff and landing being done using rocket thrust, the stall speed is important because the higher the stall speed, the more rocket propellant is expended while accelerating to that speed. From these considerations, a stall speed of 115 kts [213 km/hr] and a cruise speed of 150 kts [278 km/hr] were selected. Future optimization will refine these selections.

The initial gross weight[11] for this rapid design study was selected as 6,000 lbs [2722 kg] based on an educated guess of "10 times the payload plus some more." This, applied to the wing loading required to meet the stall speed, leads to a total wing area of 1929 sqft [179 sqm] which was increased to 2080 sqft [193 sqm] to add some margin. An aspect ratio of 57 was selected to minimize drag and keep the chord length relatively short, given the large area. The wing was developed as two panels, an untapered inner section and a 2-to-1 tapered outer section. RDS^{win} was used estimate an equivalent trapezoidal planform for aerodynamic reference (see Fig. 2). For the initial layout, a NASA laminar flow airfoil was used but this is just a placeholder pending design of a custom airfoil tailored to the flight environment. To provide adequate ground clearance on irregular Martian terrain, the wing and propellers must be mounted far above the fuselage.

	[FPS]				[MKS]			
	Wing-Inboard	Wing-Outboard	Wing - Aero Reference	Vertical Tail	Wing-Inboard	Wing-Outboard	Wing - Aero Reference	Vertical Tail
Area Sref	1000	1080	2079.3	20	92.9	100.34	193.17	1.86
Aspect Ratio	20	38.401	57.221	3.2	20	38.401	57.221	3.2
Taper Ratio	1	0.5	0.526	1	1	0.5	0.526	1
Sweep (LE)	0	0.995	0.714	0	0	0.995	0.714	0
Sweep (c/4)	0	0.497	0.402	0	0	0.497	0.402	0
Thickness t/c	17.50%	17.50%	17.50%	15%	17.50%	17.50%	17.50%	15%
Span	141.421	203.649	344.934	8	43.105	62.072	105.136	2.438
Root Chord	7.071	7.071	7.903	2.5	2.155	2.155	2.409	0.762
Tip Chord	7.071	3.535	4.154	2.5	2.155	1.078	1.266	0.762
Mean Chord	7.071	5.5	6.222	2.5	2.155	1.676	1.897	0.762
Y-bar	35.355	45.255	77.295	4	10.776	13.794	23.56	1.219

Figure 2 Top View with Wing Planform Parameters [metric on right]

The next design challenge was the arrangement of the propulsion systems. Four electric motors and propellers were initially assumed, seeking a compromise between redundancy and simplicity. Two of them are placed far outboard on the wings in nacelles which extend to the rear as tail booms. The other two are near to the vehicle centerline and in a pusher configuration to keep them away from the cabin pressure vessel in case of blade loss. Their nacelles extend forward creating a place for the vertical thrust rocket engines (8 in number, so that loss of any one can be balanced by shutting off its opposite number). These nacelles are also used as the structural tie-ins for the wing struts. Propellant tanks are located in the wing, near the rocket engines. Flat battery packs for the inboard electric motors are located just outboard of the propellant tanks. For the outboard electric motors, the battery packs are also in the wing and just inboard of their nacelles. This outboard location provides a span-loading benefit to reduce wing structural weight.

[11] When not specified, all weights listed here should be assumed to be surrogates for "mass" and representing the force values if measured on Earth. These are adjusted for the lesser gravity on Mars when used in lift calculations and the like.

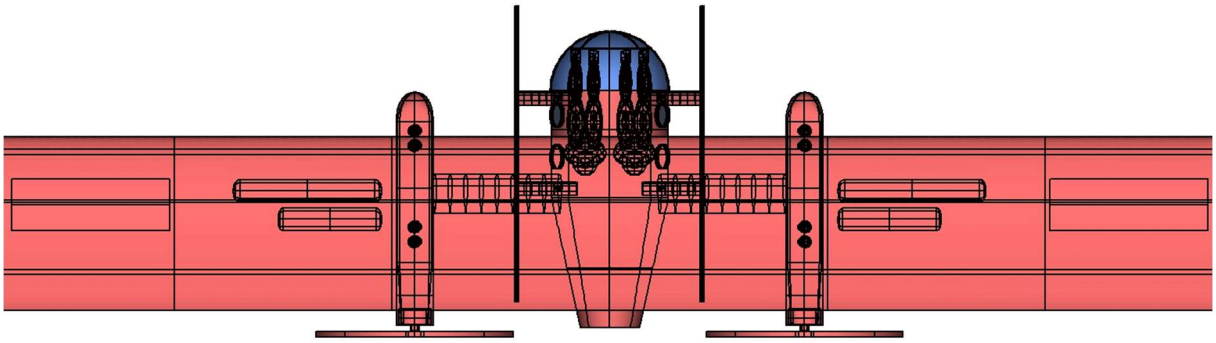

Figure 3 RMMP-1 Center Section Top View

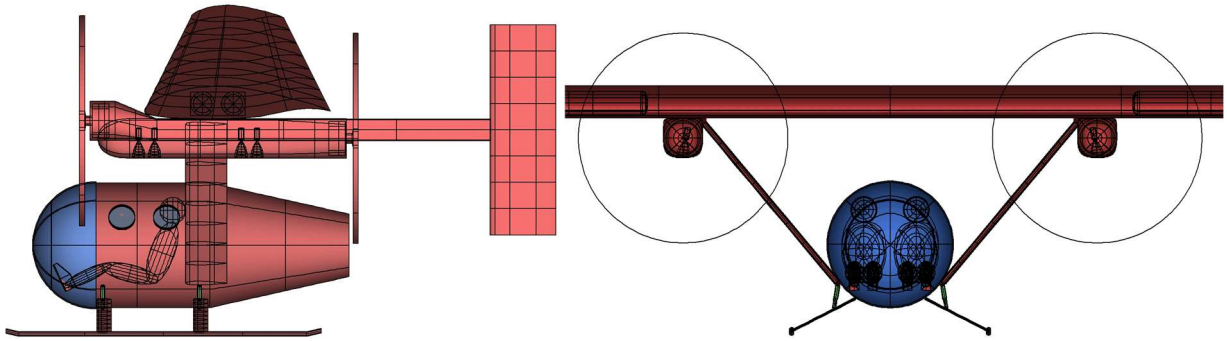

Figure 4 RMMP-1 Side & Front Views

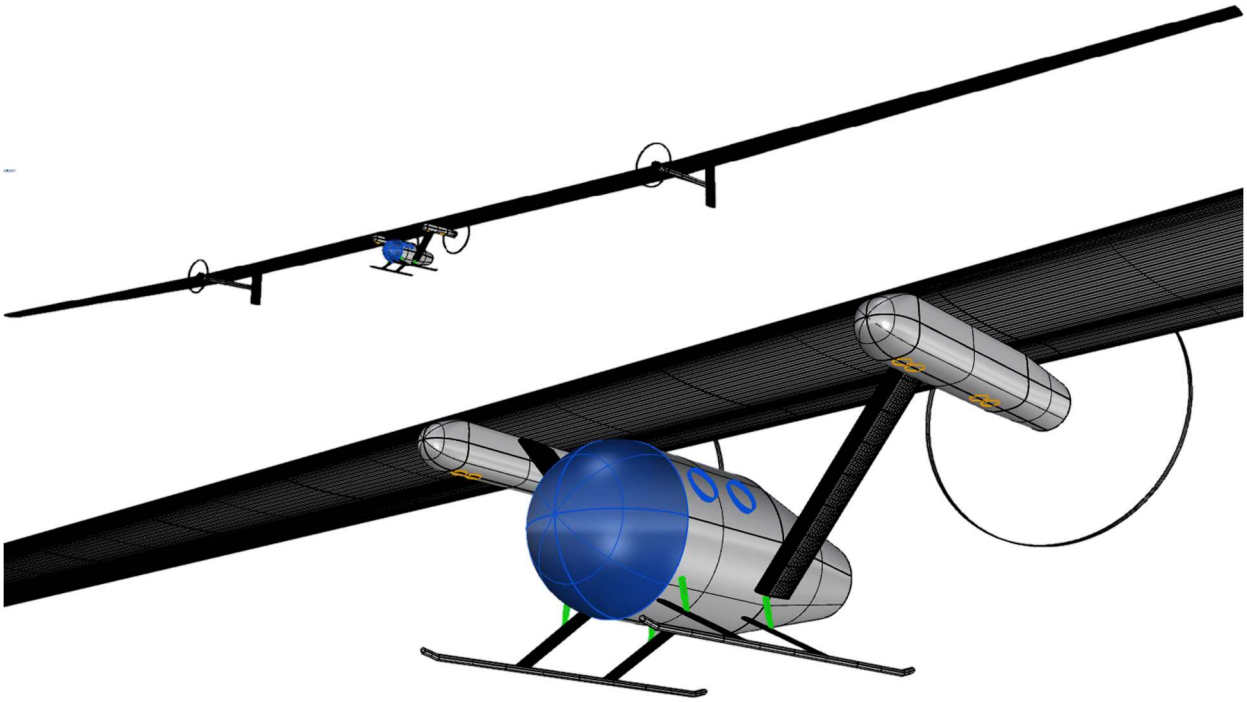

Figure 5 RMMP-1 Perspective

For the initial concept layout, small vertical tails were provided with the intention of making the design neutrally stable in yaw. These are fixed and there would be no rudders. Yaw control would be provided by differential thrust from the electric motors, automatically keeping zero sideslip in all conditions. No horizontal tail was provided. It was

assumed that with the center of gravity positioned properly, an active flight control system could provide pitch stability. It was later learned that the desirable airfoils had such a large pitching moment that a horizontal tail was probably needed, and so was provided on the second design iteration as described below.

Primary structure is assumed to be fabricated from the most advanced composites in the 2030 timeframe, expertly done such that the highest system properties are obtained. Beyond the classical 1.5 factor of safety, minimal extra design margins would be applied.

V. Baseline Vehicle Preliminary Analysis

An initial aerodynamic analysis was done using the classical routines of the RDS^{win}-Pro aircraft design software[7]. Luckily the atmosphere model in RDS^{win} goes up to orbit for aerospace plane analysis, but these results must be viewed with caution due to the extreme low Reynold's Number of the Martian flight condition. Also, no adjustment was made for differences due to the different chemical composition of the air on Mars.

With those caveats, the subsonic parasite drag was estimated by the component buildup method. Typical skin roughness was assumed, along with substantial credit for laminar flow. A base drag penalty was added for the flat back end of the fuselage, pending a trade study on a more-streamlined but harder to build fuselage. Drag due to lift was calculated by the leading-edge suction method using a calculated Cl-alpha based upon DATCOM methods, with the leading-edge suction schedule adjusted for the high aspect ratio wing. A wing design lift coefficient of 0.7 was assumed.

Aerodynamic results are summarized below as lift-to-drag ratio. Typical flight speeds are about Mach 0.25, so the best L/D would be just over 40, at a lift coefficient of 0.78. Later CFD analysis showed this to be optimistic due mostly to Reynolds Number effects on the airfoil properties (see below).

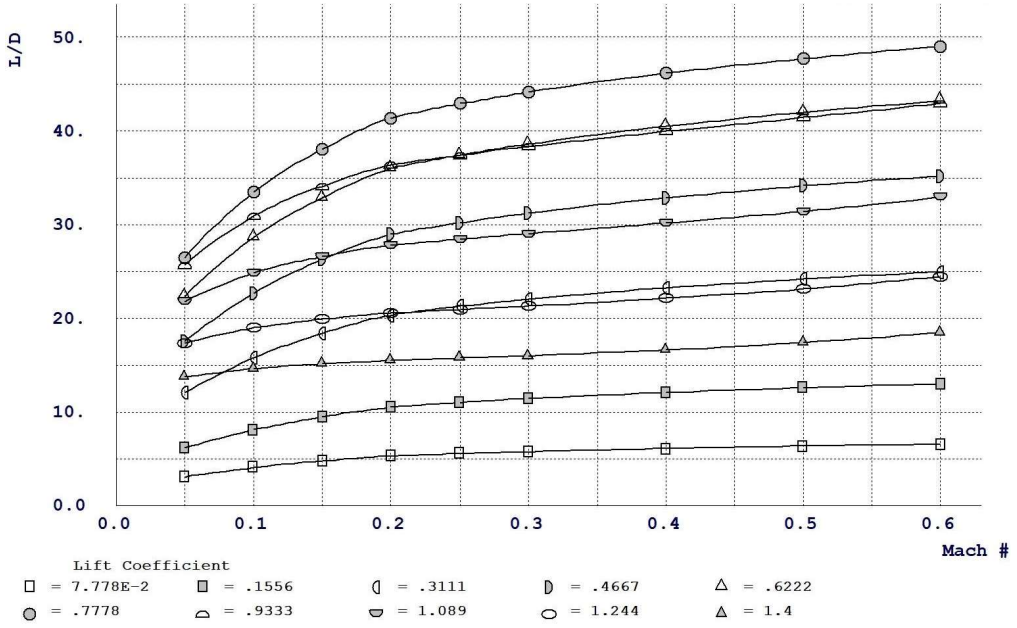

Figure 6 RMMP-1 Lift-to-Drag Ratio

Given the strangeness of this design, its extreme aspect ratio, its flight environment, and the non-standard local force of gravity, the normal statistical weights estimation equations as contained in RDS^{win} could not be used. Instead the lead author estimated component weights using estimated weight-per-unit-area, adjusted actual component weights, and outright guesses. Subsequent analysis by the international volunteer team seems to support those numbers.

Weights are calculated here as Earth equivalent weight force. Results are tabulated below, and show that a gross weight of 6,000 lbs [2722 kg] yields an empty weight of about 4,112 lbs [1865 kg] which, less payload and rocket propellant, leaves a net available weight for batteries of about 834 lbs [378 kg].

	Weight	Loc	Moment		Weight	Loc	Moment
	lbs	ft	ft-lbs		lbs	ft	ft-lbs
STRUCTURES	**2732.0**		**18641**	**EQUIPMENT**	**640.0**		4220
Wing	1871.4	7.2	13556	Flight Controls	40.0	5.5	220
Vertical Tails	30.3	18.4	559				0
Wing Struts	125.0	6.4	806				0
Passenger Pod	253.3	4.1	1048	Electrical (incl actuators)	100.0	6.0	600
Fuselage (rest of)	75.2	9.2	695	Avionics	20.0	5.0	100
Canopy	73.8	1.5	109	Pressurization and AC	80.0	5.0	400
Nacelle Inbd	78.2	7.3	569	Solar Cells & equip	300.0	7.0	2100
Nacelle Outbd	73.5	7.5	551	Furnishings & Equipment	100.0	8.0	800
	0.0		0				
	0.0		0	(% We Allowance)	5.0		
Landing Gear	151.3	4.9	748	Empty Weight Allowance	195.8	6.8	1329
PROPULSION	**544.3**		**3719**	**TOTAL WEIGHT EMPTY**	**4112.1**	**6.8**	27909
Electric Motors (4)	52.2	7.0	368				
Motor Installation	40.0	7.0	282	**USEFUL LOAD**	**1887.9**		
Engine Controllers	41.8	7.0	294	Crew	400.0	4.1	1640
Propeller	40.0	7.0	280	Battery Wt available	834.1	7.0	5839
Battery Installation	200.0	7.0	1400				0
	0.0		0	Rocket propellant	553.8	7.0	3877
Rockets (8)	82.3	6.3	514	Payload	100.0	6.4	640
Rocket Installation	48.0	6.3	300				
Propellant tanks	40.0	7.0	280	**TAKEOFF GROSS WEIGHT**	**6000.0**	**6.7**	39905

	Weight	Loc	Moment		Weight	Loc	Moment
	kg	m	kg-m		kg	m	kg-m
STRUCTURES	**1239.2**		**2577**	**EQUIPMENT**	**290.3**		583
Wing	848.8	2.2	1874	Flight Controls	18.1	1.7	30
Vertical Tails	13.8	5.6	77			0.0	0
Wing Struts	56.7	2.0	111			0.0	0
Passenger Pod	114.9	1.3	145	Electrical (incl actuators)	45.4	1.8	83
Fuselage (rest of)	34.1	2.8	96	Avionics	9.1	1.5	14
Canopy	33.5	0.5	15	Pressurization and AC	36.3	1.5	55
Nacelle Inbd	35.5	2.2	79	Solar Cells & equip	136.1	2.1	290
Nacelle Outbd	33.3	2.3	76	Furnishings & Equipment	45.4	2.4	111
	0.0	0.0	0				
	0.0	0.0	0	(% We Allowance)	5.0		
Landing Gear	68.6	1.5	103	Empty Weight Allowance	88.8	2.1	184
PROPULSION	**246.9**		**514**	**TOTAL WEIGHT EMPTY**	**1865.2**	**2.1**	3859
Electric Motors (4)	23.7	2.1	51				
Motor Installation	18.1	2.1	39	**USEFUL LOAD**	**856.4**		
Engine Controllers	18.9	2.1	41	Crew	181.4	1.2	227
Propeller	18.1	2.1	39	Battery Wt available	378.3	7.0	2648
Battery Installation	90.7	2.1	194				0
	0.0	0.0	0	Rocket propellant	251.2	2.1	536
Rockets (8)	37.3	1.9	71	Payload	45.4	2.0	88
Rocket Installation	21.8	1.9	41				
Propellant tanks	18.1	2.1	39	**TAKEOFF GROSS WEIGHT**	2721.5	**2.7**	7358

Figure 7 RMMP-1 Weight Analysis (FPS above, MKS below)

The range and flight time of the Raymer Manned Mars Plane (RMMP-1) was calculated by spreadsheet analysis as shown below, using equations from *AD:ACA*[8]. The most uncertain of the inputs are the L/D estimated using RDS[win] and the propeller efficiency, for which a typical value of 0.8 was assumed. Luckily the estimated range is far in excess of the required value so that even the reduced L/D values found by the CFD below should leave sufficient range for the basic "Jeep" mission.

Range (Level Flight):			
mb/m = battery mass fraction	**0.1367**	for cruise	
Esb = battery energy density {wh/kg}	**500**	260	
ηb2s = efficiency -battery to motor shaft	**0.9**		
ηp = propeller efficiency	**0.8**		
L/D	**42**		
Range {km}	**1999.3**	**1079.5**	nmi
Velocity {km/h} -not needed for Range calc	**277.8**	150.0	kts
Motor Power Used P/W {Watt/g}	**0.0085**	0.0052	hp/lb
time	**7.20**		

Figure 8 RMMP-1 Range Analysis

A similar calculation estimated the rate of climb. Given the relatively low power-to-weight ratio, the slow rate of climb is not unexpected. This should not be a problem when flying in the relatively flat northern hemisphere of Mars, but additional motor power and/or supplemental rocket thrust may be required to safely fly in the mountainous regions of the southern hemisphere.

Climb Vertical Velocity	
Velocity {km/h}	**277.8**
Motor Power Used P/W {W/g}	**0.0318**
ηb2s = efficiency -battery to motor shaft	**0.9**
ηp = propeller efficiency	**0.8**
L/D	**42**
Vertical Velocity {m/s}	**4.997**
Vertical Velocity {fpm}	**983.5**

Figure 9 RMMP-1 Climb Analysis

Early in this design study it was imagined that landing would best be done by a deep stall maneuver, allowing the vehicle to drop vertically only to be arrested by rocket thrust at the "last second." Analysis indicates that in a deep stall, the thin air would allow the vehicle to reach a terminal speed of 246 fps [75 mps]. Even with double the rocket engines thrust required for level flight, it would take 18 seconds and 2200 feet [670 m] to check the downward velocity. Since cruise will often be at a lower altitude, the deep stall approach doesn't seem viable. Instead the vehicle will slow down in level flight, transfer weight from the wings to rocket thrust, and making a vertical landing.

VI. Revised Baseline Concept RMMP-2

After the work described above was presented to the AIAA "New Space" online conference, a volunteer team began to work on the project. Results are described below and contributed to the modifications to the initial design as described in this section.

One thing learned in CFD analysis was the criticality of Reynolds Number on drag and lift. While not unexpected, the severity of this effect drove a change in wing layout, with aspect ratio reduced from 57 to 25 mostly to increase the wing chord R#. This reduces parasitic drag but at some penalty to drag due to lift. The reduction in aspect ratio reduces span as well as increases chord length and thickness, with a happy side benefit of improving structure.

To avoid a reduction in chord length at the wingtip, the revised wing has no taper. Since this tends to load up the wingtip, a bit of twist was added. This will also tend to avoid tip stall which can be exacerbated by the low R#. To mitigate the drag due to lift of an untapered planform, a raked wingtip with both sweep and dihedral was added. This also increases dihedral effect which allows some roll control using differential thrust to create a slight yaw.

The NASA NLF(1)-0215F had been used as a placeholder for the initial layout, with full expectation of replacing it with a bespoke airfoil. A new airfoil, denoted FF-RMMP150-12, was designed and is described in a section below. Like most optimal airfoils designed to such flight conditions, it has a lot of camber near the trailing edge. This leads to large pitching moments which must be countered. Rather than rely on extreme actuation of a control surface at the trailing edge it was decided to add horizontal tails. These were positioned at the back of the tail booms, aft of the fixed vertical tails and half-way out the wingspan. At this location it should be possible to use differential deflection to twist the wing for roll control but this has not been analyzed.

Other design changes included lengthening the inboard nacelles to move their aft-facing propellers farther away from the wing trailing edge, and moving the outboard nacelles closer to the vehicle centerline since the wingspan is reduced. Rocket engines were added to the outboard nacelle to provide more-positive roll control during takeoff and landing. Later analysis may show that these are not required.

The structural analysis as described below demanded an increase in the thickness and chord length of the two wing struts which connect the wing to the fuselage. These changes combined led to the revised configuration shown below:

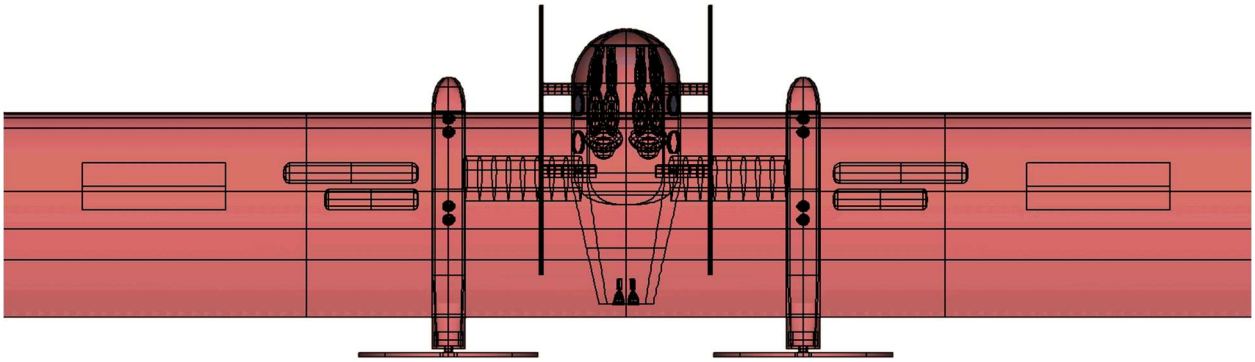

Figure 10 RMMP-2 Center Section Top View

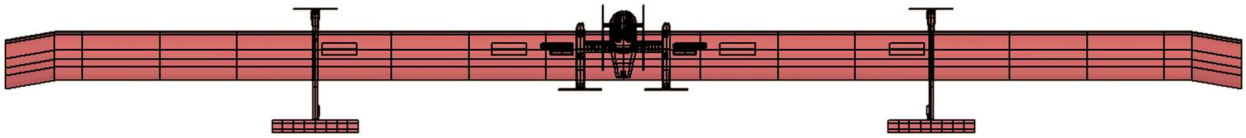

Figure 11 RMMP-2 Top View and Wing Planform

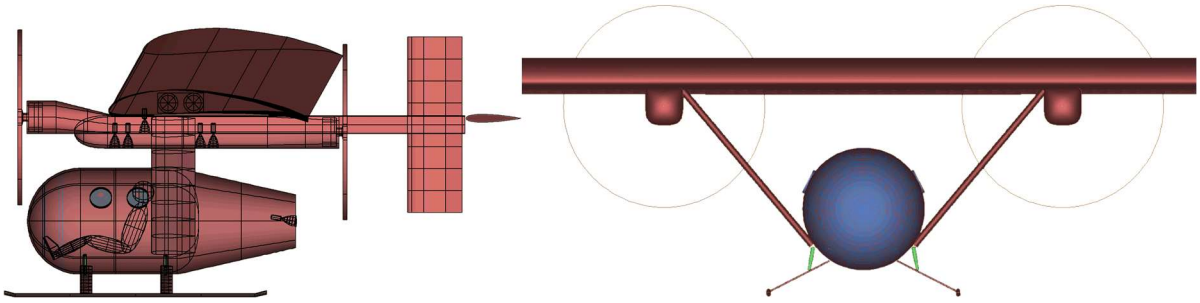

Figure 12 RMMP-2 Side & Front Views

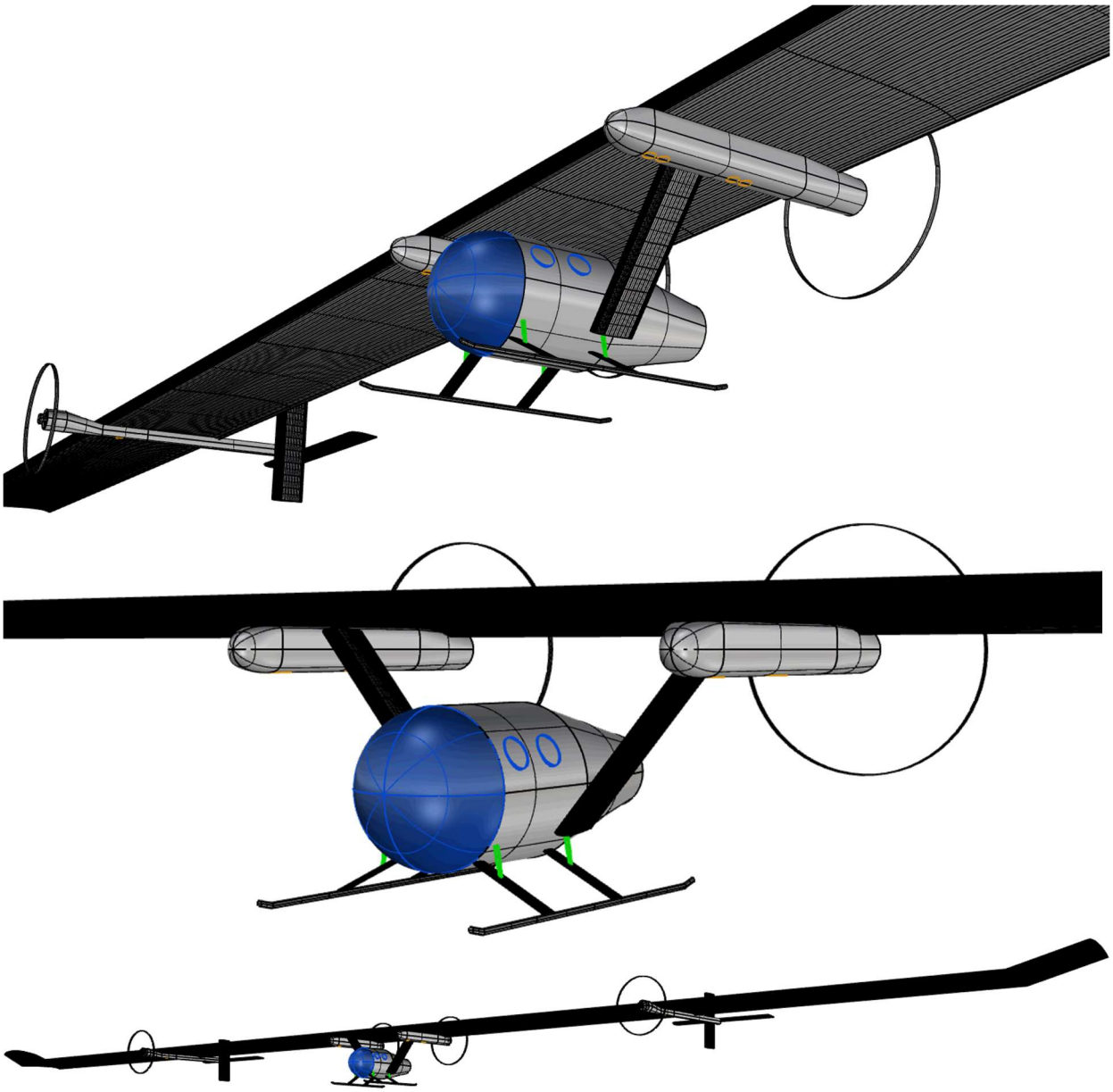

Figure 13 RMMP-2 Perspectives

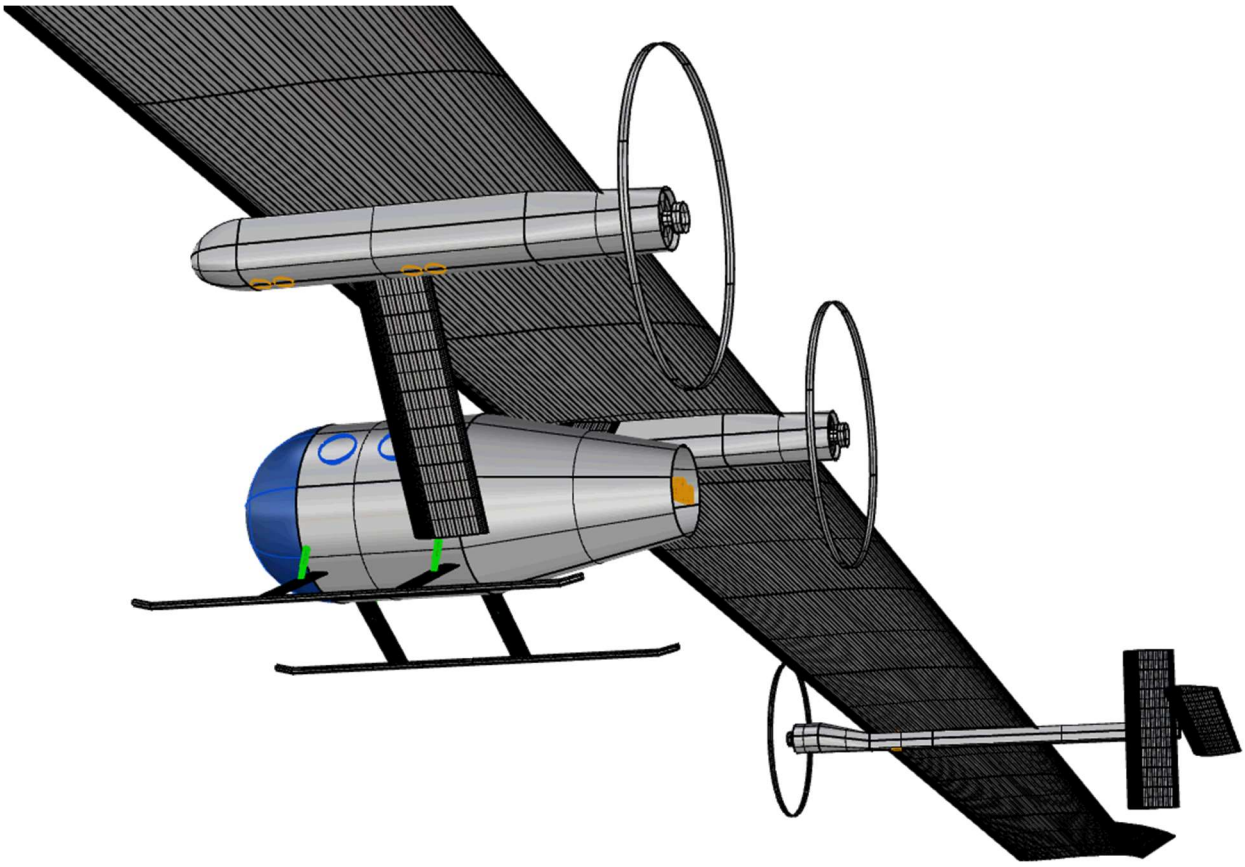

Figure 14 RMMP-2 In Flight

	[FPS]			[MKS]		
	Wing	Vertical Tail	Horizontal Tail	Wing	Vertical Tail	Horizontal Tail
Area Sref	2080	20	40	193.24	1.86	3.72
Aspect Ratio	25	3.2	6.4	25	3.2	6.4
Taper Ratio	1	1	1	1	1	1
Sweep (LE)	0	0	0	0	0	0
Sweep (c/4)	0	0	0	0	0	0
Thickness t/c	0.12	0.15	0.15	0.12	0.15	0.15
Dihedral	0.00	0.00	0.00	0.00	0.00	0.00
Incidence	2.50	0.00	0.00	2.50	0.00	0.00
Twist	-2.00	0.00	0.00	-2.00	0.00	0.00
Span	228.035	8	16	69.505	2.438	4.877
Root Chord	9.121	2.5	2.5	2.78	0.762	0.762
Tip Chord	9.121	2.5	2.5	2.78	0.762	0.762
Mean Chord	9.121	2.5	2.5	2.78	0.762	0.762
Y-bar	57.009	4	4	17.376	1.219	1.219

Figure 15 RMMP-2 Wing Planform Parameters

The following sections describe the work done by the international team of volunteers. Most of their work was done on the initial RMMP-1 baseline but in some cases, they were able to rerun their analysis once the RMMP-2 configuration was completed. Following these analysis sections is a Summary and Conclusion.

VII. Aerodynamics and Airfoil Design

(Felix Finger, FH Aachen Univ. of Applied Sciences, Germany)

3D Aerodynamic Analysis

To assess the aerodynamic performance, the RMMP-1 was analyzed using steady-state RANS simulations. The aircraft was analyzed for two flow conditions: 2° angle of attack (AoA) at MSL and 2° AoA at 150,000 ft, which is representative of the flow conditions on Mars. At this early design stage, no attempt was made to precisely model Mars' atmosphere in CFD. The simulation at MSL conditions (high Reynold's number) was performed as a reality check, against which the RDSwin drag numbers could be compared. The simulation parameters for both flow conditions are shown below:

3D RANS simulation parameters

Parameter	MSL	105k ft
Free stream velocity V_∞ [m/s]	66	77.17
Reference pressure p_∞ [Pa]	101.325	867.5
Density ρ_∞ [kg/m3]	1.225	0.01322
Dynamic viscosity μ [Pa·s]	$1.812 \cdot 10^{-5}$	$1.4869 \cdot 10^{-5}$
Reynold's number Re [-]	$9.593 \cdot 10^{6}$	$0.142 \cdot 10^{6}$
Turbulence intensity (inlet) [-]	1%	1%
Turbulent viscosity ratio (inlet) [-]	10	10

The simulation was set up according to the recommendations outlined in Götten[10]. The RANS equations were solved using the assumptions of incompressible flow, and the SST k-ω (Menter) turbulence model was used. The bullet-shaped flow field was divided into finite volumes using an unstructured cartesian cut cell mesher with a dedicated prism mesh, which discretizes the boundary layer. Boundary layer thickness for each aircraft part and both flow conditions was determined, ensuring y^+ values below 1 on all aircraft's surfaces. The surface mesh size was adjusted to give approximately 70 cells over the wing in chordwise direction. To decrease the computational effort, a half-model was used, and a symmetry condition was applied. To reduce the cell count, the landing gear was excluded from the model. These measures resulted in a domain size of 21 Mio cells, which represented the maximum possible cell count on the available workstation. Due to this memory limitation, a mesh independence study was not carried out.

The results for both flow conditions are presented below. These allow one to draw some interesting conclusions: in both cases wing drag (which includes induced drag) is dominant, making up more than 90% of the total drag. At sea level the L/D is as high as expected, but the low Reynold's number at 105k ft reduces L/D by more than 50%. The placeholder airfoil (NASA NLF-1) is unsuited for these flow conditions.

3D RANS results

Parameter	MSL 2deg AoA	105k ft 2deg AoA
C_L	0.891	0.749
$C_{D\ total}$	0.01823	0.03456
L/D	48.88	21.67
$C_{D\ Wing}$	0.01679	0.03200
$C_{D\ Nacelle\ inner}$	0.00032	0.00052
$C_{D\ Nacelle\ outer}$	0.00011	0.00028
$C_{D\ Fuselage}$	0.00055	0.00095
$C_{D\ Struts}$	0.00021	0.00045
$C_{D\ Vertical\ tails}$	0.00025	0.00036

The following conclusions were drawn from this initial study: The aerodynamic design of the RMMP must be driven by the wing's design because the drag of all other components is negligible compared to the wing's drag. The very low Re-number on Mars dictates the use of a custom airfoil to reduce flow separation and drag.

2D Aerodynamic Analysis

A review of low Reynold's number airfoils revealed a lack of high lift airfoils for the flight conditions of the RMMP. Airfoils for human-powered airfoils were considered, but most were optimized for Re > 200,000. Therefore, a new airfoil needed to be developed for the RMMP. This problem was approached by coupling the well-known XFoil code to a multipoint shape optimization routine. The numerically optimized airfoils were then further modified manually to improve the pressure distributions.

While XFoil is a great tool to quickly analyze and compare airfoils, it is lacking in the prediction of drag when compared to a 2D RANS method. Therefore, candidate airfoils were analyzed using a 2D RANS method. Turbulence was simulated with Menter's SST model, and the γ-Re_θ-model is used to simulate boundary layer transition. The 2D flow domain was discretized into 350,000 cells.

At the Reynold's number of the Dash-1 RMMP design, maximum airfoil L/D values ranged from 38 at 16% t/c to 54 at 10% t/c. The low Re conditions take their toll. The target L/D of 44 was not achievable with such limited airfoil performance. The design needed to be changed to obtain better performance. Consequently, it was decided to increase wing Reynolds number by increasing wing chord and the design speed to 150% of the Dash-1 values. A reduction in aspect ratio would allow using an airfoil with a 12% thickness ratio, which is considered a great starting point for further aero-structural optimization.

The optimization process was rerun for the new set of requirements. The resulting airfoil (FF-RMMP150-12) is shown below along with its performance. With a maximum L/D > 60, this airfoil should provide much-improved performance over the initial placeholder airfoil and is therefore chosen for the Dash-2 design.

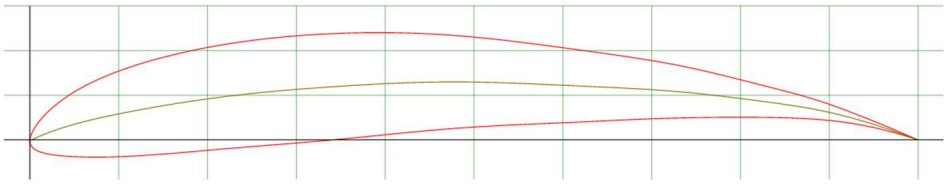

Figure 16 FF-RMMP150-12. Max thickness 12% at 30.1% chord. Max camber 6.5% at 48.4% chord

FF-RMMP150-12. 2D RANS results

AoA [deg]	Cl [-]	Cd [-]	Cm [-]	L/D [-]	$L^{1.5}/D$ [-]
-2.5	0.4762	0.01883	-0.1879	25.3	17.5
0.0	0.7366	0.01542	-0.1859	47.8	41.0
2.5	1.0046	0.01682	-0.1835	59.7	59.9
5.0	1.2603	0.02070	-0.1820	60.9	68.4
7.5	1.4625	0.02601	-0.1729	56.2	68.0
9.5	1.5713	0.03257	-0.1597	48.2	60.5
11.0	1.5883	0.04289	-0.1463	37.0	46.7

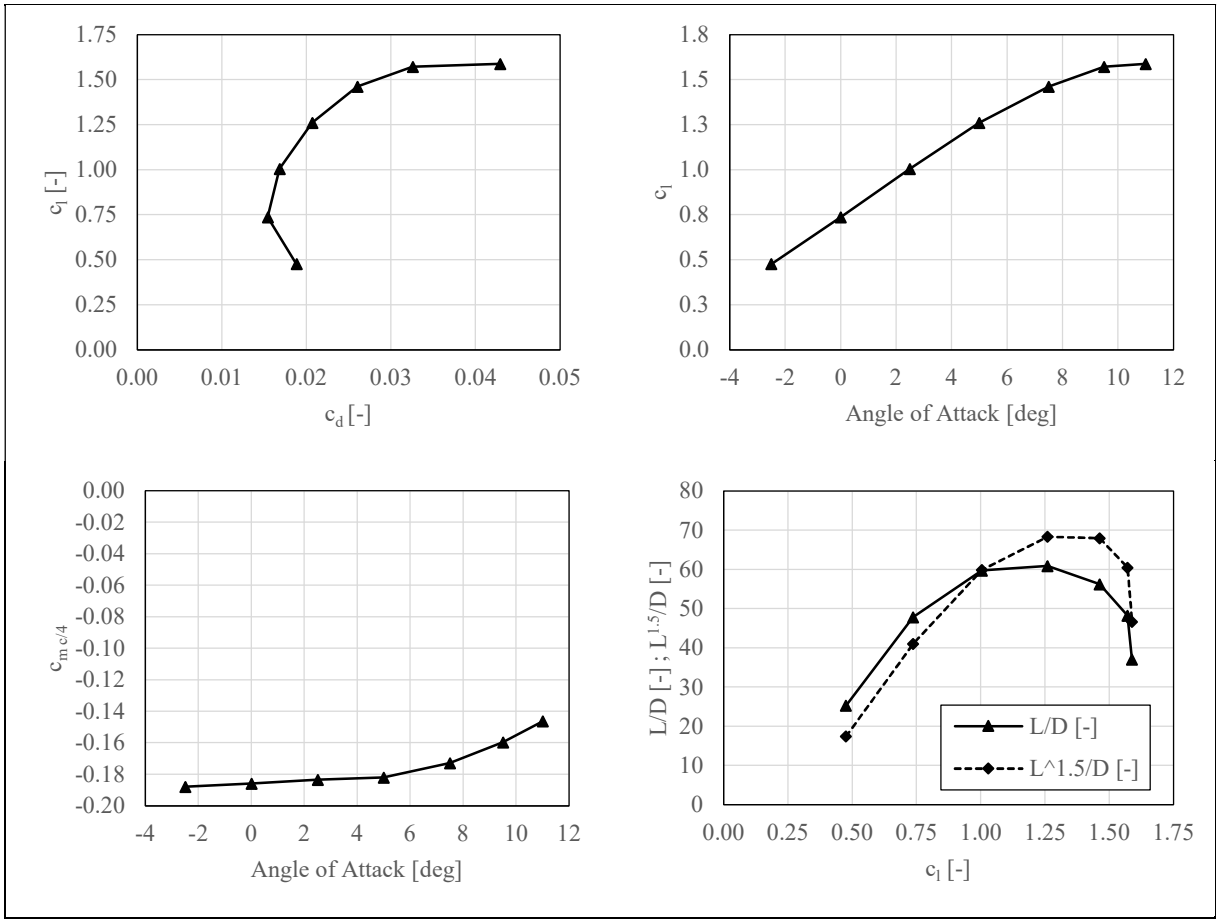

Figure 17 FF-RMMP150-12. Aerodynamic performance

VIII. Structural Design & Analysis

(Arturo Gomez, University Carlos III of Madrid, Spain)

A preliminary wing structure architecture is proposed to ensure that the wing-box can support limit loads without permanent deformation and that the deformation is maintained within the limits for safe operation. The wing is mainly supported by a central wing box structure with two spars (FWD ad AFT) at 20% and 60% of the chord respectively and 45 ribs located along the span including two heavy ribs to reinforce the strut-wing attachment and two for the out nacelle. The distance between ribs is shorter in the inboard section in order to prevent structural instability in this heavily loaded region. The strut is made from a single cell box that transfer bending and torsion loading from the passenger's compartment into the wing's heavy ribs.

All structural components are made with composite sandwich construction with stacking sequence and material that vary depending on the structural component and the loading requirements. Carbon Fiber Reinforced Plastics (CFRP) HexTow HM63/8552 is chosen as the main structural material due to its high specific stiffness. Divinycell foams (HP60 & HP100) are used as a core material due to its low weight and relatively high strength and stiffness. The total weight of the aircraft's wing-box is 762 Kg that corresponds to 84% of the available weight for the wing structure.

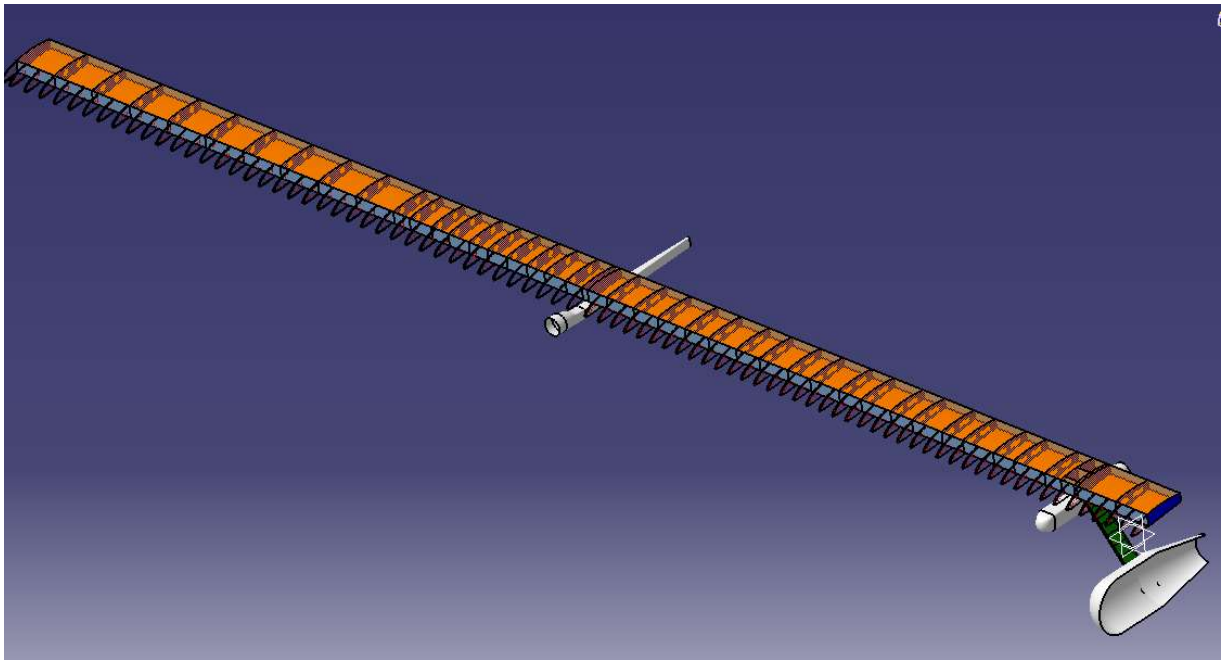

Figure 18 RMMP Wing-box Architecture

A static FEA model and a linear perturbation buckling analysis is developed in Abaqus V.6.14 to verify that the proposed wing-box structure satisfies with the strength requirements and determine if there is structural instability that could compromise the integrity of the structure. The structure is modelled with deformable 2D shell elements with reduced integration. The average mesh size is 30mm for 45617 elements in total. Composite laminates are modelled following to the corresponding stacking sequence using three integration points per ply.

All wing-box components are connected using a tie constraint. External loads (airloads and rockets trust) are placed in equilibrium with inertial forces using inertial relief boundary condition. For this, approximate weight distribution in the span-wise direction is introduced through non-structural masses at different rib locations. The lift distribution is assumed to be perfectly elliptical and approximated by four-step distributions along the span which are applied as surface traction in the skin top surface. Displacements and rotations (U2, UR1, UR3) are restrained in the root due to symmetry around the mid-plane.

Four loading conditions are considered: i) level flight at stall speed (n=1), ii) symmetric (+) maneuvers (n=2.5), iii) symmetric (-) maneuvers (n=-0.8) , iv) steady take-off at full rocket trust (T=10675 N).

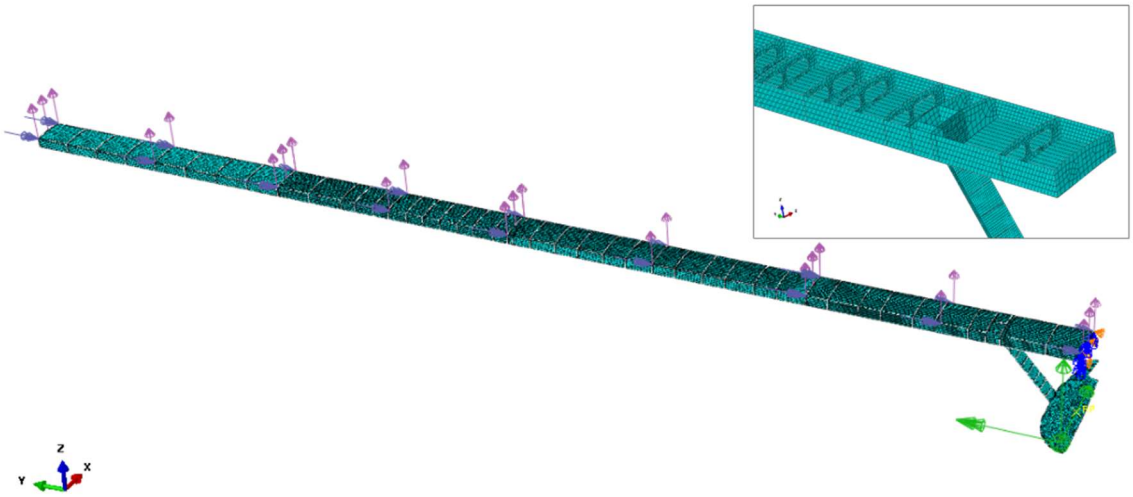

Figure 19 FEA Model and Mesh

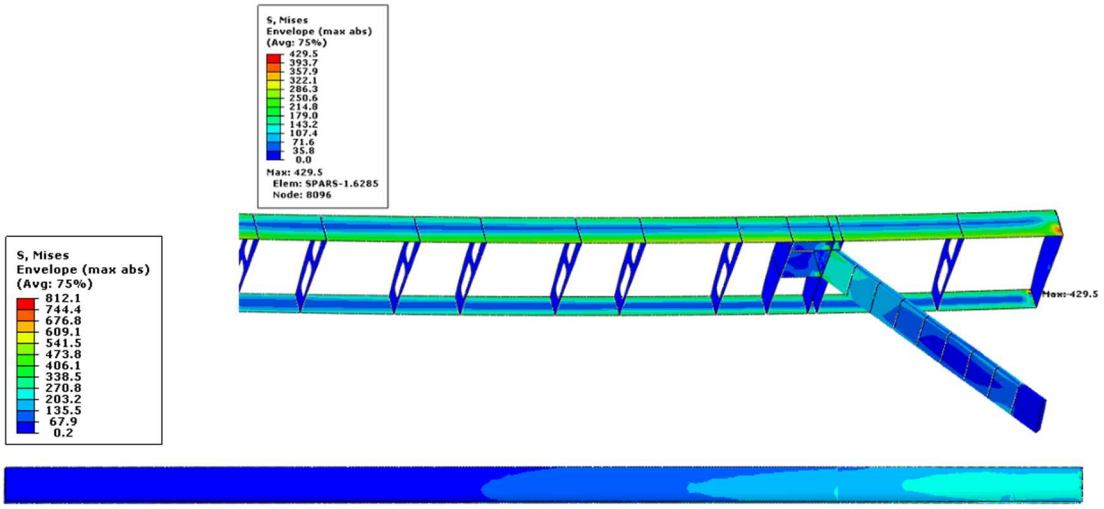

Figure 20 Stress distribution Case I

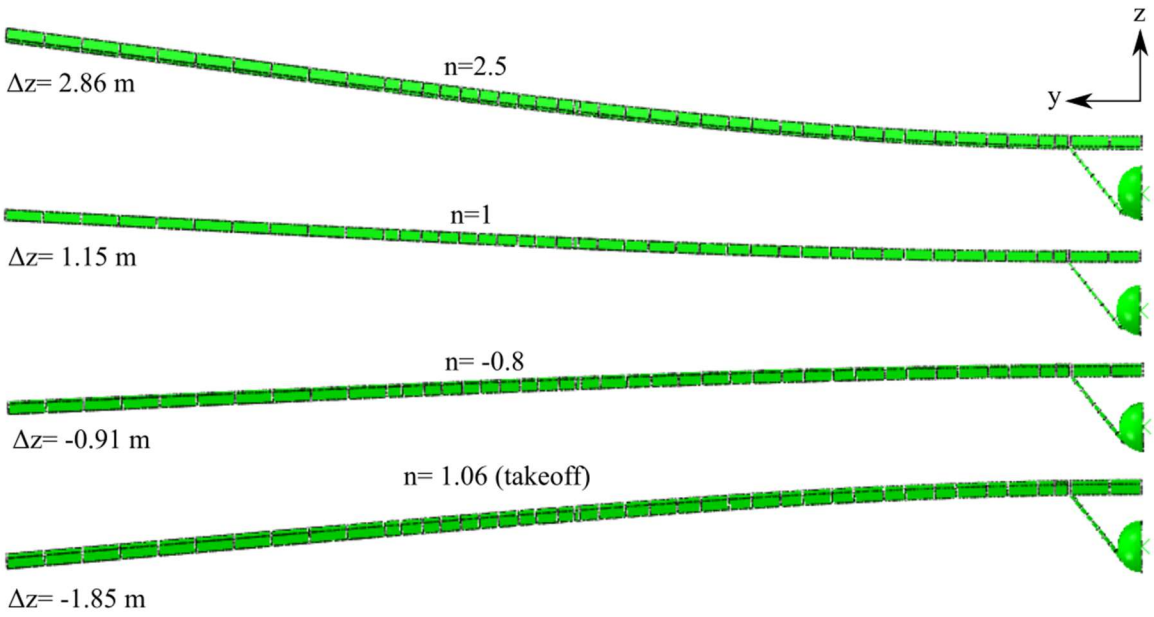

Figure 21 Tip Deflections

For all the analyzed conditions, the wing complies with the strength requirements and no structural instability is present. The wing-tip deflection is particularly high and it could compromise the normal operation of flight control surfaces and massively modify the aerodynamic response of the airplane. To get the correct results, we should include the effect of the wing deformation in the aerodynamic analysis.

The following table summarizes the results obtained from the FEA model.

Case	n (g)	σ_{max} (Mpa)	Δz_{tip} (m)	$Hashin_{max}$	λ_1	Permanent deformation?	Structural Instability?	Comment
0	1	112.3	1.15	0.14		NO	NO	Steady level flight at Vs
I	2.5	279.8	2.868	0.86	1.0278	NO	NO	(+) symmetric at Va
II	-0.8	89.28	0.248	0.02	3.458	NO	NO	(-) symmetric at Va
III	1.06	201.2	0.536	0.11	1.23	NO	NO	Steady take-off with rockets

This analysis assumes use of today's best composite materials and takes no credit for any future improvement in the characteristics of the materials or in design methods, fiber arrangements, or fabrication methods. One can expect that materials will massively improve by 2030 particularly with the improvement of filaments, thermoplastic resins, nanocomposites, and out of autoclave processes. Since the weight goals are met with current technologies, no credit was taken but should be assessed in a detailed study.

IX. Stability and Control Analysis

(Ramlingam Gyanasampath Pillai, University of Texas at Arlington)

A key factor in the design of a Manned Mars Airplane is the attainment of acceptable static stability and control. The RMMP-1 baseline configuration was analyzed using the Vortex Lattice Method in the OpenVSP software developed by NASA. Following this analysis, two other configurations were defined and analyzed to help decide upon viable improvements to the baseline configuration especially in light of the high-camber airfoils which were emerging from the aerodynamics studies. One of these has horizontal tails added to the twin tail booms. This was considered but not included in the original RMMP-1 baseline. With differential deflection these would function as ailerons and are so labeled in the charts below, but here aeroelastic effects are not included. In all likelihood this deflection would twist the wings so much that the net roll would be in the opposite direction – potentially useful!

The second alternative configuration has a single horizontal tail stretching from tail boom to tail boom, a total distance of 140 ft [43 m]. This unlikely "single bar" configuration was studied just to quickly consider some alternative to the two-separate-tails approach. Had it proven superior, a configuration with tail booms moved far inwards could have been considered.

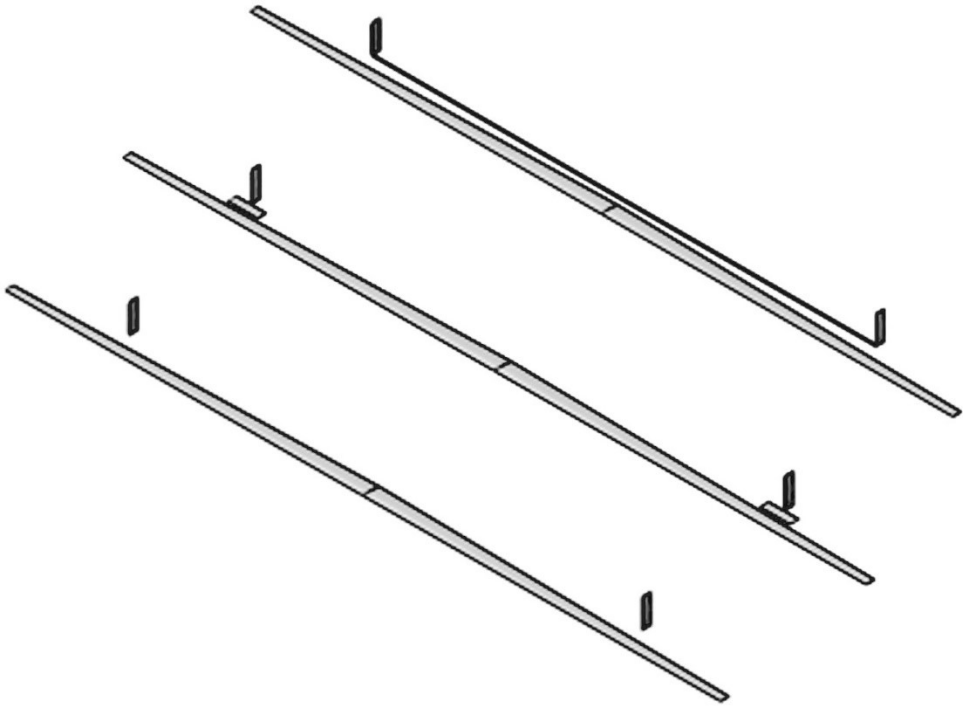

Figure 22 S&C Trade Study Configurations: Baseline, "Ailerons", & "Single Bar"

Longitudinal stability results for the baseline and two alternatives are presented below. As expected, the tailless configuration is unstable and would rely upon an active flight control system. Both aft-tail configurations are stable. The pitching moment graph includes results for the RMMP-2 configuration, showing that it is stable in pitch thanks to the addition of horizontal tails on the ends of the tail booms.

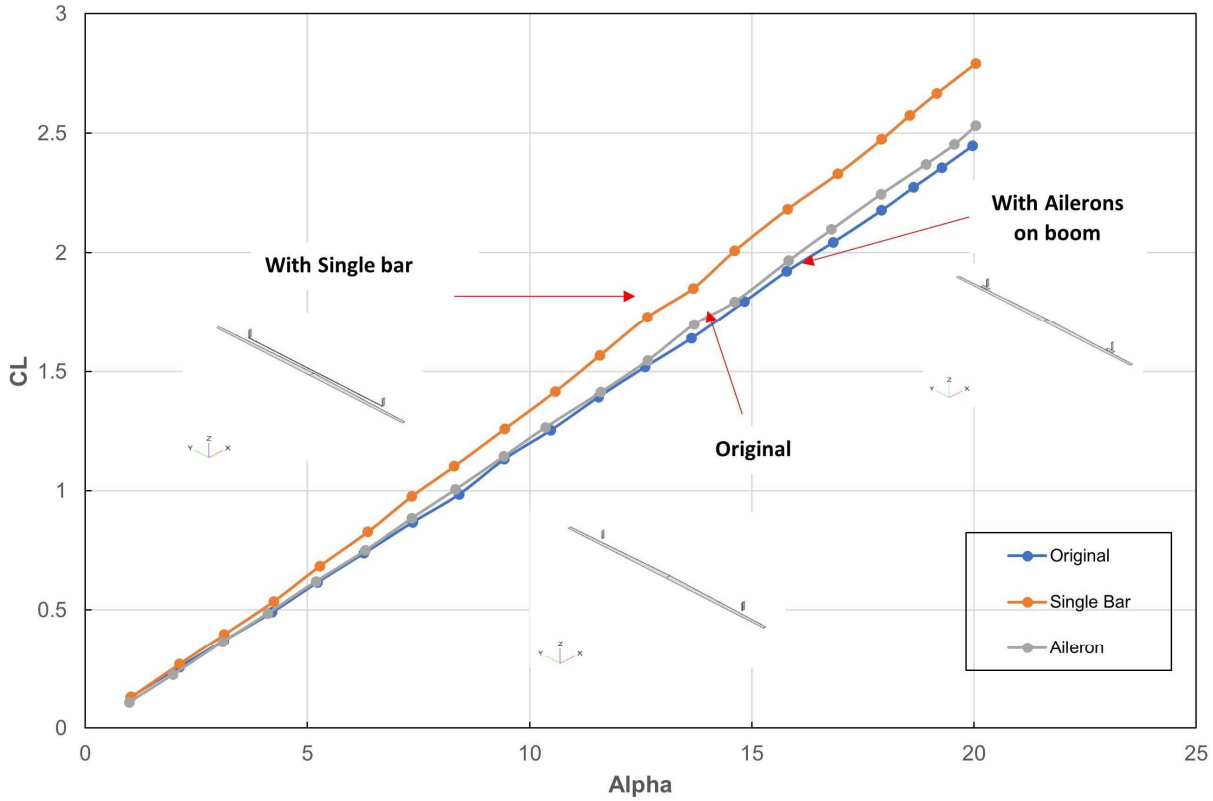

Figure 23 Lift Coefficient vs. AOA

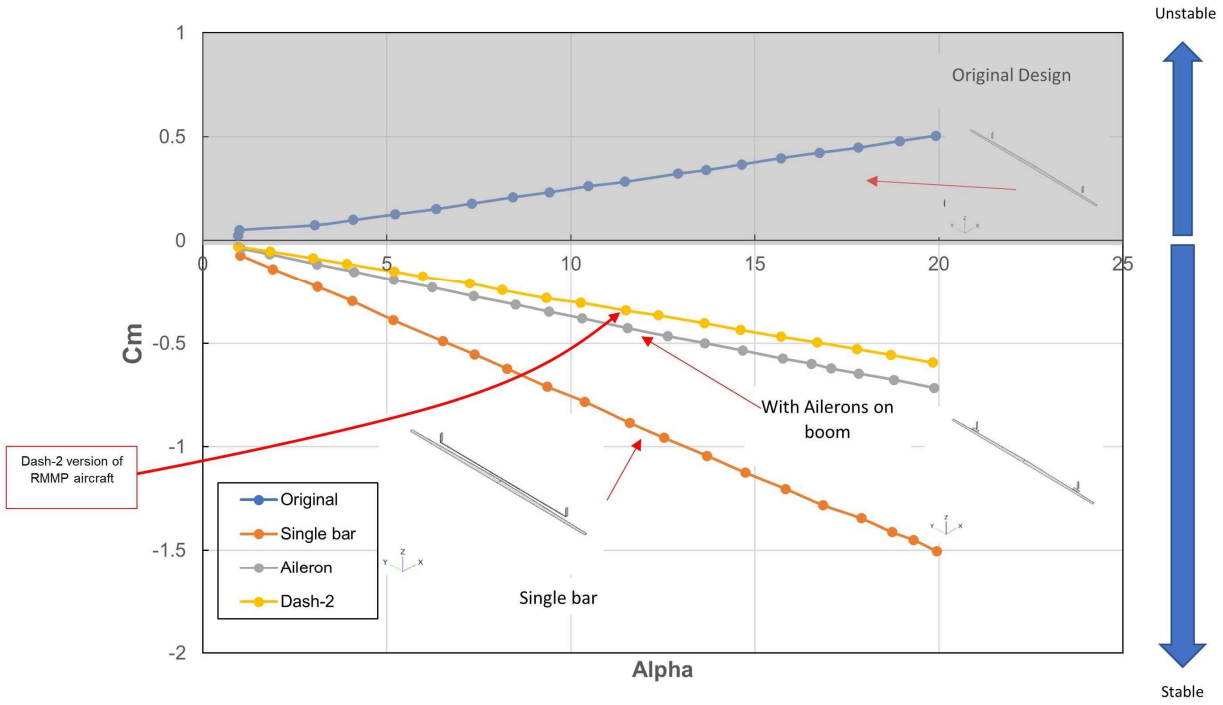

Figure 24 Pitching Moment vs. AOA

In terms of yawing moment, the vertical tail spanwise location is surprisingly important for lateral stability. To map these characteristics a vertical tail spanwise location factor has been defined for trade study purposes as the percent distance between the two vertical tails divided by the total wingspan. For wingtip-mounted tails this would be 100%. The baseline RMMP-1 has a factor of 41%. Analysis results are shown below where a positive $C_{n\text{-}beta}$ is a stable aircraft. Results indicate that tip tails are fine at low angles of attack but lose stability at higher AOAs. Other tail locations stay close to neutrally stable as desired. Later the RMMP-2 configuration was analyzed and, on this graph, yields a nearly flat line at zero yawing moment indicating neutral yaw stability, as desired.

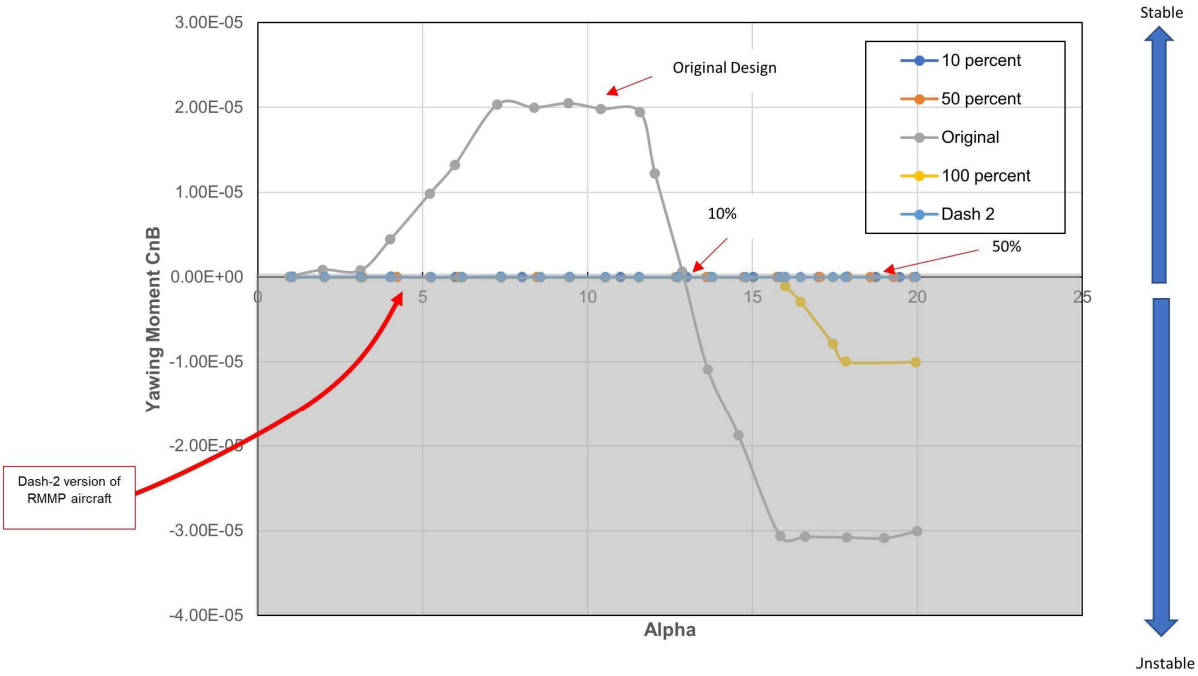

Figure 25 Yaw Stability

To avoid excessive response to wind gusts, it is desirable for the RMMP to have near-neutral rolling moment response (dihedral effect). The next figure shows that the original design and the version with horizontal tail "ailerons" on the tail booms both have this exact characteristic, as does the revised RMMP-2 design. For some reason the design with the long "single bar" tail stretched between the tail booms shows a greater response but it is still small in total magnitude.

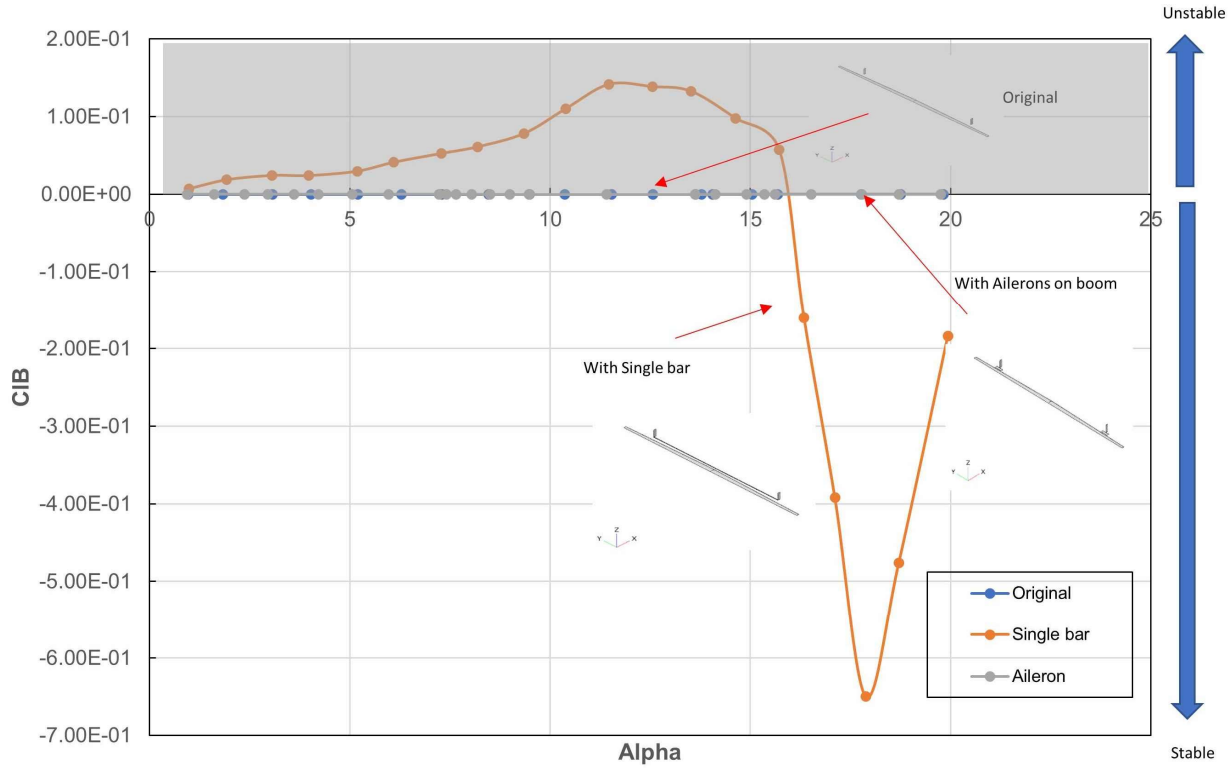

Figure 26 Roll Stability

X. Takeoff and Transition Analysis

(Matheus Monjon, Federal University of ABC, Sao Paulo, Brazil)

The takeoff modeling was implemented with MATLAB, using standard mechanics equations (F=Ma, etc...). The analysis ran from time t=0 on the ground, to the time when the vehicle achieves sustainable flight, namely speed is greater than stall speed.

Propeller thrust was estimated using actuator disk theory using the given diameter. Rocket thrust was given as 300 lbs [1334 N] for each of eight vertical thrust engines and two horizontal thrust engines. To avoid excess vertical accelerations, a thrust control function was implemented to reduce vertical rocket engine thrust after ground clearance. The vehicle drag coefficient was estimated from a vortex lattice method plus a parasitic drag contribution.

Simulation results are shown below, first for the case where horizontal rocket engines are used to speed the acceleration to flight speed, and next for the case where propeller thrust alone is used to accelerate.

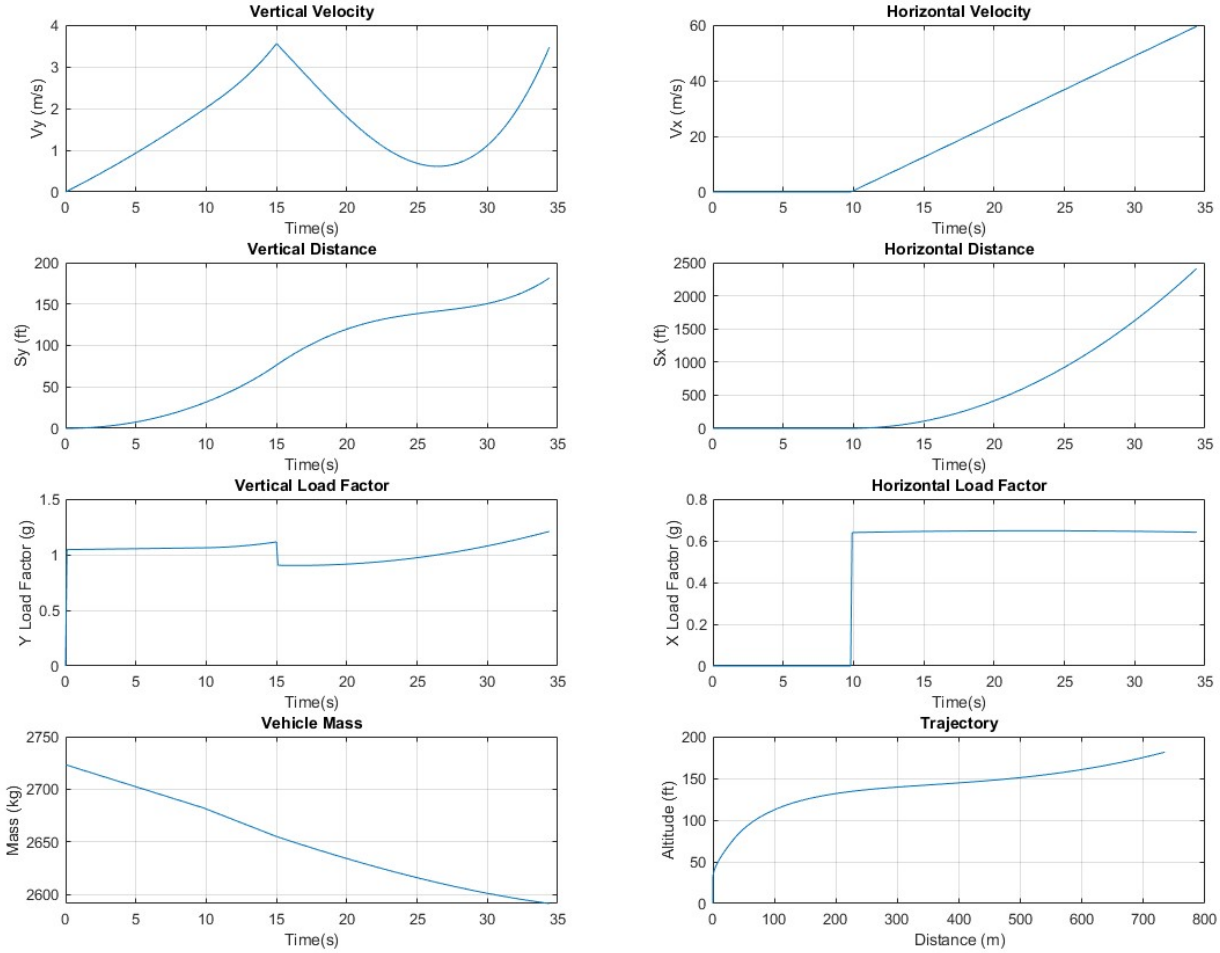

Figure 27 Takeoff Simulation With Horizontal Rocket Thrust

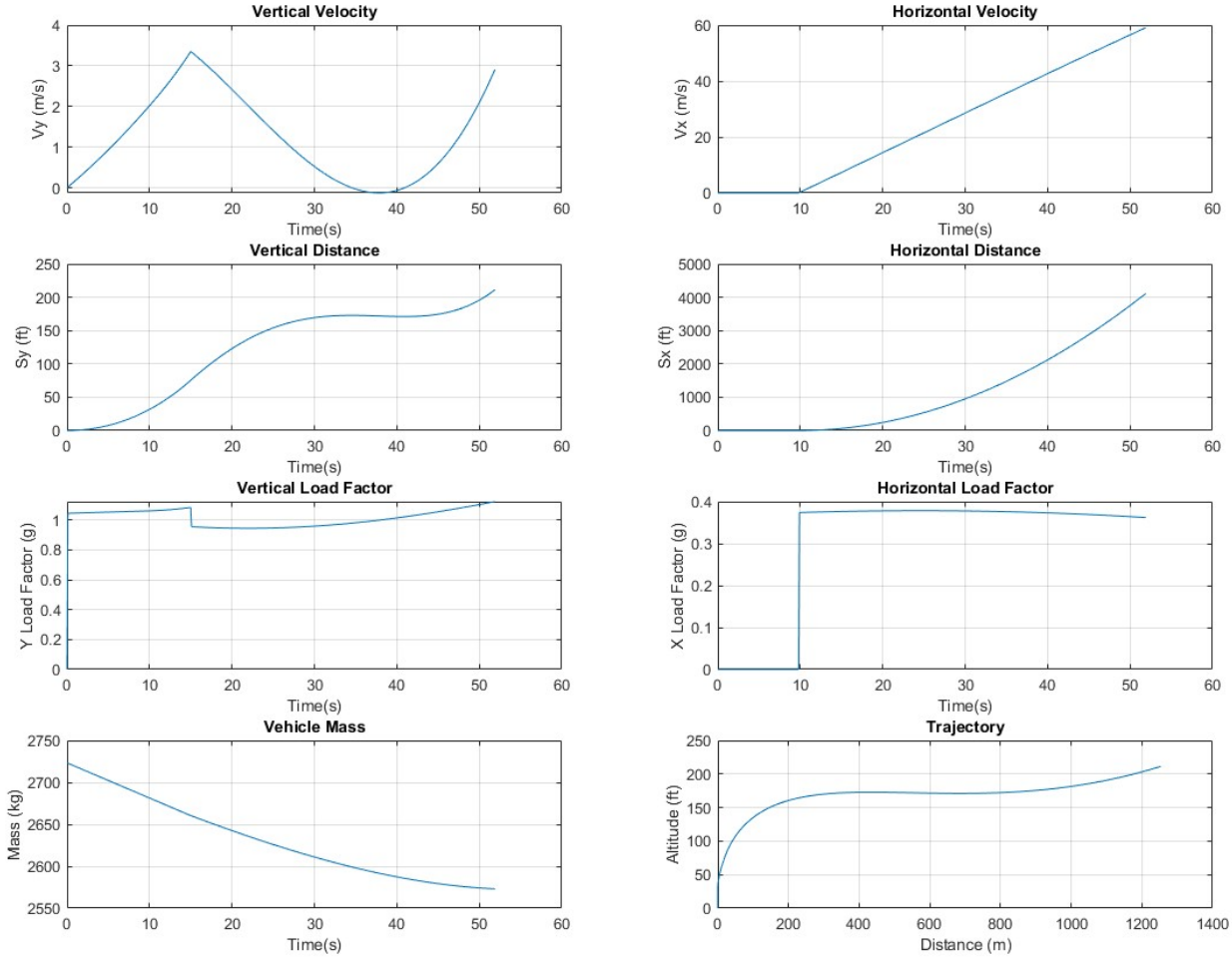

Figure 28 Takeoff Simulation Without Horizontal Rocket Thrust

The results indicate that the addition of horizontal rocket thrust does reduce the time to accelerate by a substantial amount. This reduces total propellant required despite the additional propellant required for that horizontal thrust. Without horizontal thrust the takeoff uses 331 lbs [150 kg] of propellant versus only 291 lbs [132 kg] if horizontal thrust is used.

Further study is needed, but the option of not installing horizontal thrust rockets has several advantages. It offers a reduction in complexity in the installation of horizontal rockets in the rear fuselage, mainly fuel pumps and propellant supply wires, and has a safer cabin environment for occupants. It has less maintenance and possibility of failures, too. On the other hand, the horizontal rockets do reduce propellant requirements and could be of assistance in case of propeller or electric motor failure during takeoff. They also reduce the battery energy consumed.

A final option, not investigated yet, would pivot some or all of the vertical thrust engines for forward acceleration. The weight and complexity penalties would have to be considered.

XI. Propulsion and Performance

(Joabe Marcos de Souza, University of São Paulo, Brazil)

The RMMP-1 vehicle was further analyzed for performance, including considerations for the actual Martian atmosphere. This was modeled using NASA equations obtained at *https://www.grc.nasa.gov*. Momentum Theory was then used to estimate propeller efficiency in the Martian environment as shown in the figure below. Note that

this is substantially below the 0.8 efficiency value used in the earlier vehicle range estimation, which will have a direct impact upon range.

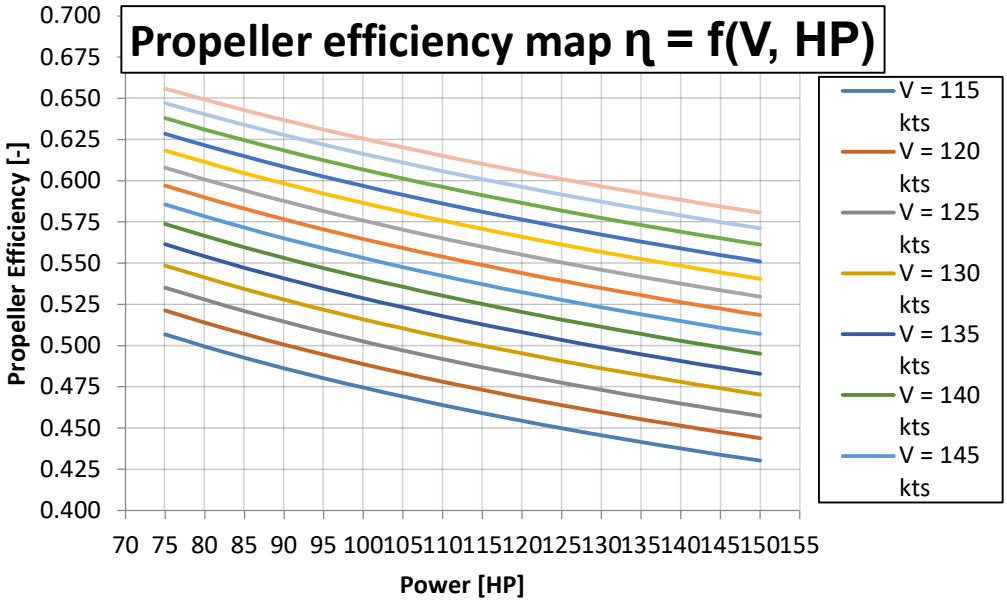

Figure 29 Propeller Efficiency Analysis

The aircraft trimmed data was estimated in order to obtain aerodynamic data as L/D and drag polar.

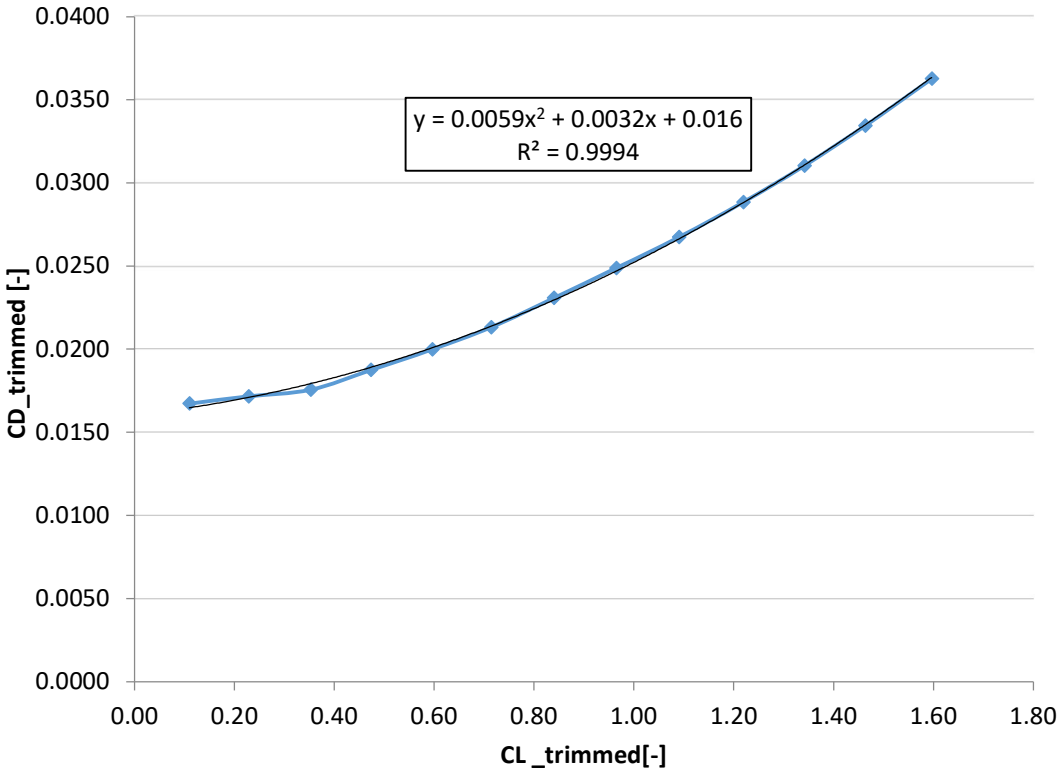

Figure 30 Trimmed Drag Estimate for Performance Calculations

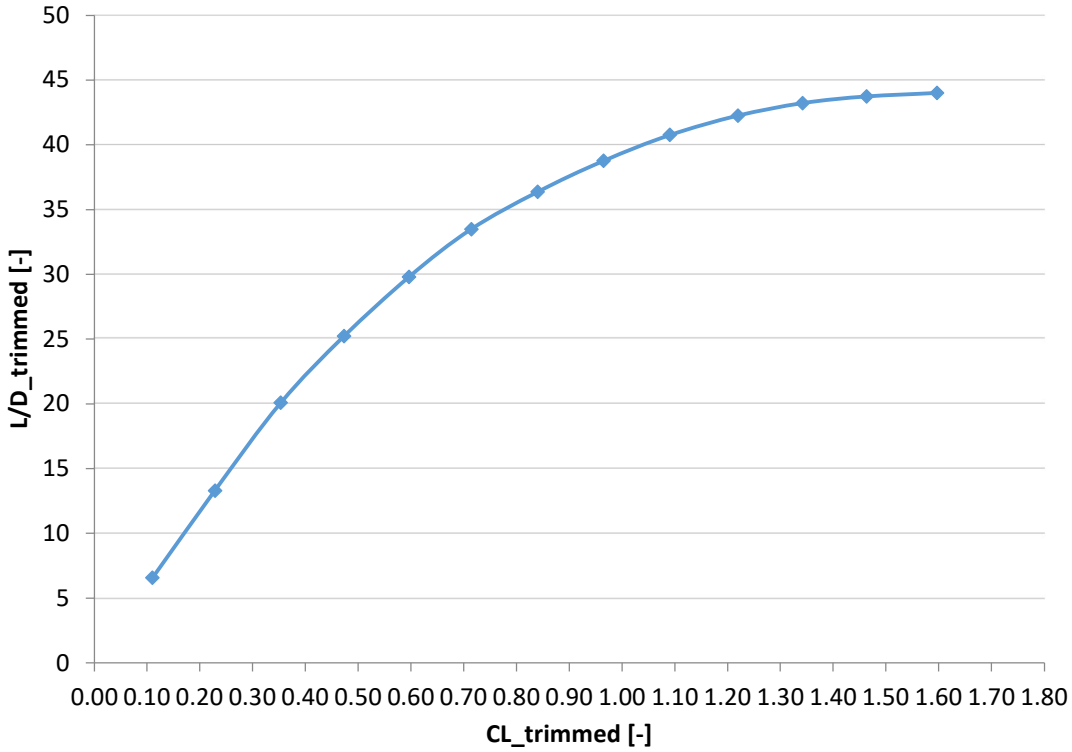

Figure 31 Trimmed L/D Estimate for Performance Calculations

A value of 90% was assumed for the total efficiency of the electric propulsion system (η_e) with an integration efficiency (η_{INT}) of 97% due installation losses. Battery specific energy of 500 Wh/kg was used which should be conservative in the 2030+ timeframe.

Using the given ratio of battery weight to takeoff gross weight (m_b/m_{TO}) equal to 0.13, a range of 669 nmi [1238 km] was obtained, cruising at a speed of 150 knots. A rate of climb greater than 3000 fpm [914 mpm] was obtained. Trade studies were done of range and speed vs. flight speed, with results as shown below.

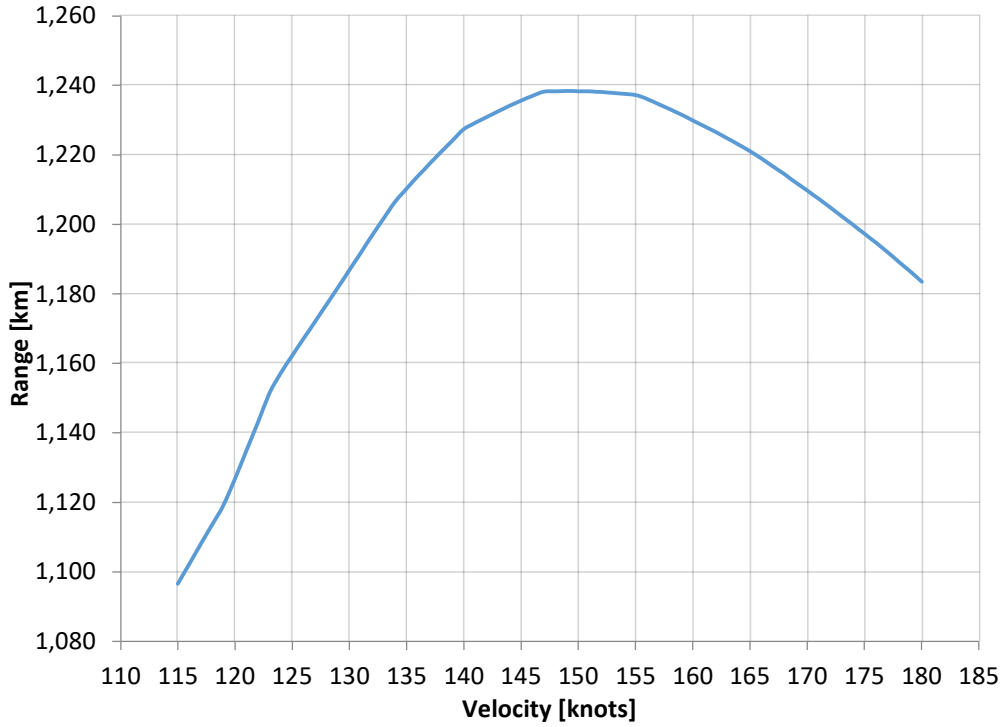

Figure 32 Velocity vs. Range Trade Study

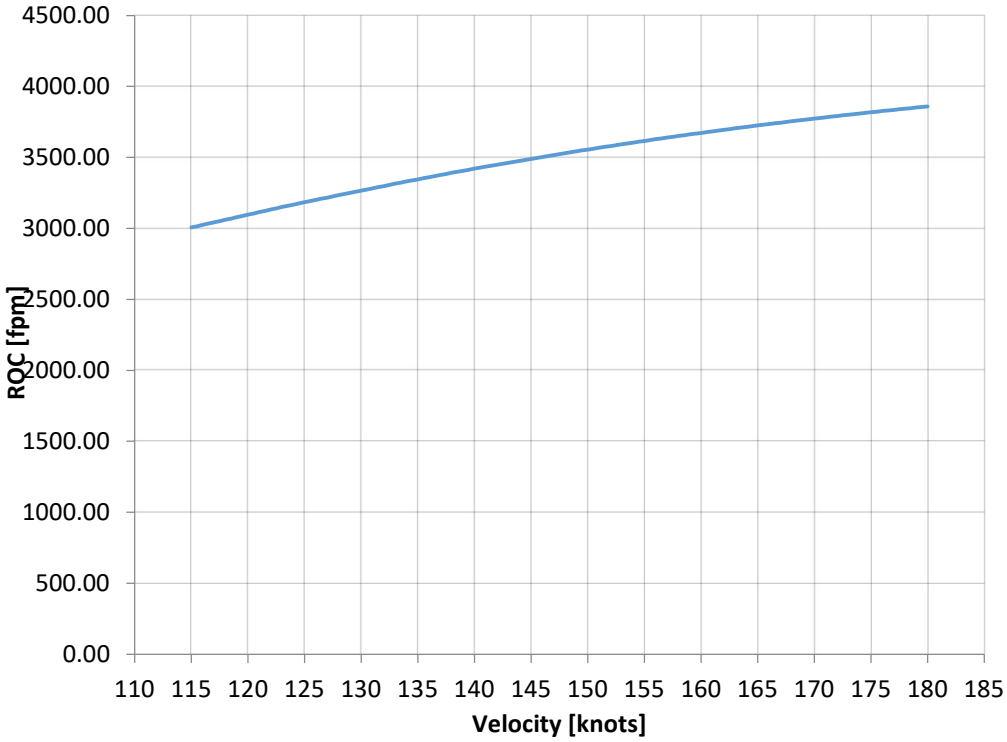

Figure 33 Rate of Climb

XII. Cabin Layout & Analysis

(analysis & interior arrangement by Jaspreet Singh, Tata Motors Ltd, India)
(interior design & renderings by Aviv Levy, Aviv Innovations, Israel)

The RMMP cabin is configured with a transparent hemispherical front-end clam shell that opens towards on one side like an autoclave door. This allows for easy ingress and egress with a step in and out cabin dimension of 4.64 ft [1.4m]. The cabin is sized to accommodate two fully suited flight crew in the global 95 percentile individual category[11].

The crew seating is sized to provide a comfortable seating space and operating envelope while minimizing frontal area for reasons of aerodynamic drag. While the original design had seats exactly side-by-side, the recommended arrangement is a staggered layout to offer more individual space to each occupant within the given cabin volume. This is enabled by fold-away panels which aid in ease of ingress and egress with the staggered layout.

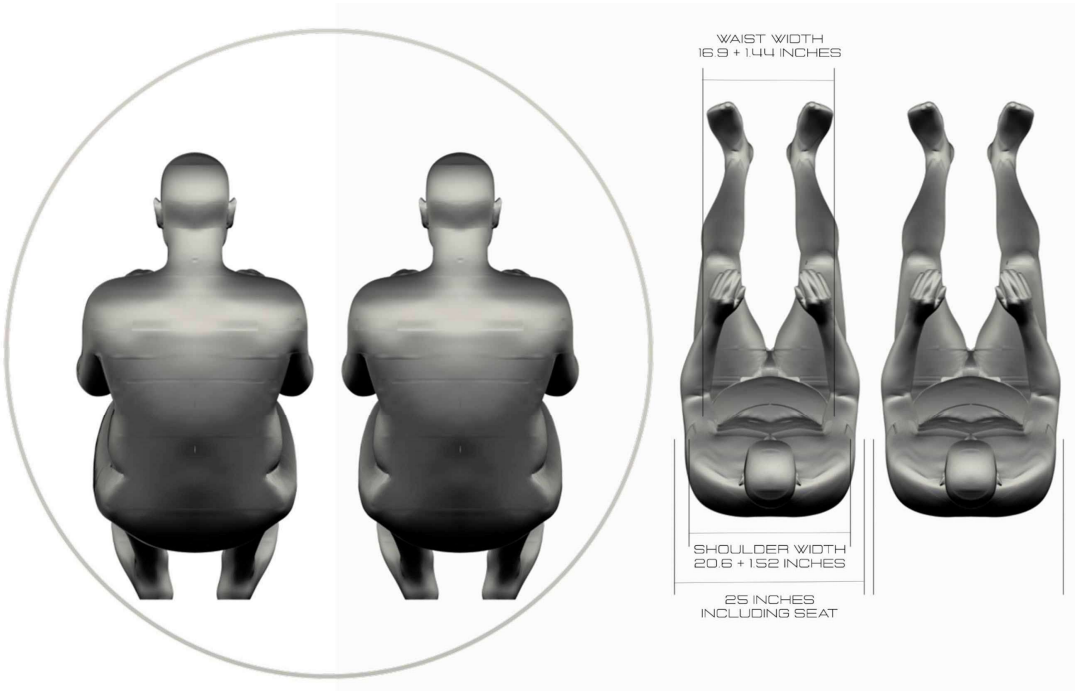

Figure 34 Cabin Layout – Side by Side

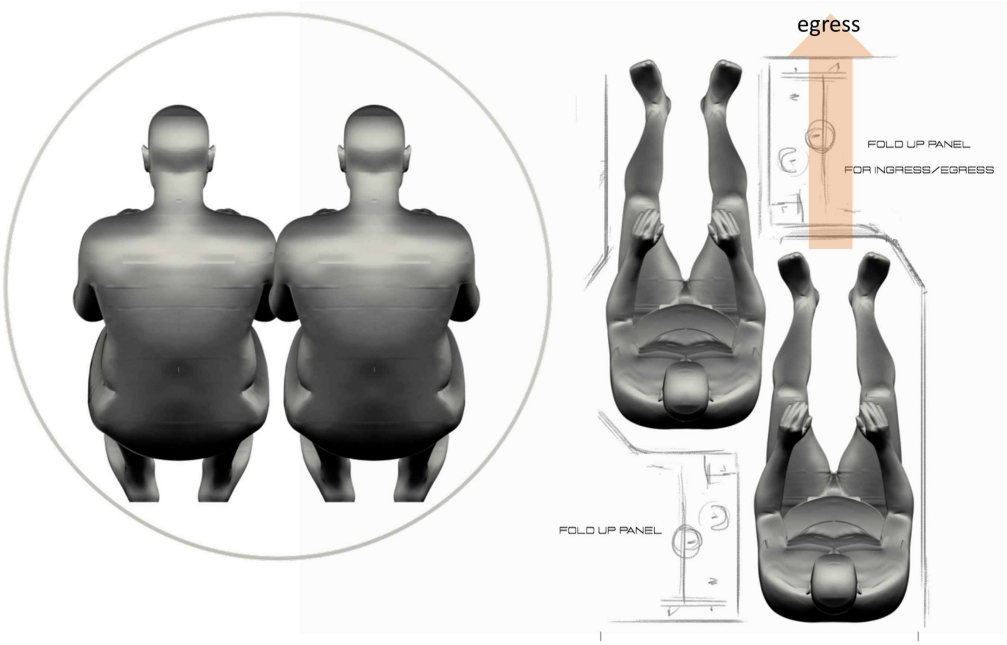

Figure 35 Cabin Layout –Staggered

The front part of the cabin is fully transparent to offer unhindered visibility to the occupants. The control gear and other accoutrements are laid-out on the sides along the fuselage walls to keep the area in between the crew free from any obstructive elements. The fuselage side walls also have port-hole type windows for side visibility. Both crewmembers are provided side stowage space for personal effects and small sized samples. The floor divides the internal volume to house ECLSS elements and the avionics bay along with other instruments.

There is a dedicated storage area with separate hatch in the rear fuselage to carry payload and samples for return. A cabin interior view is shown below.

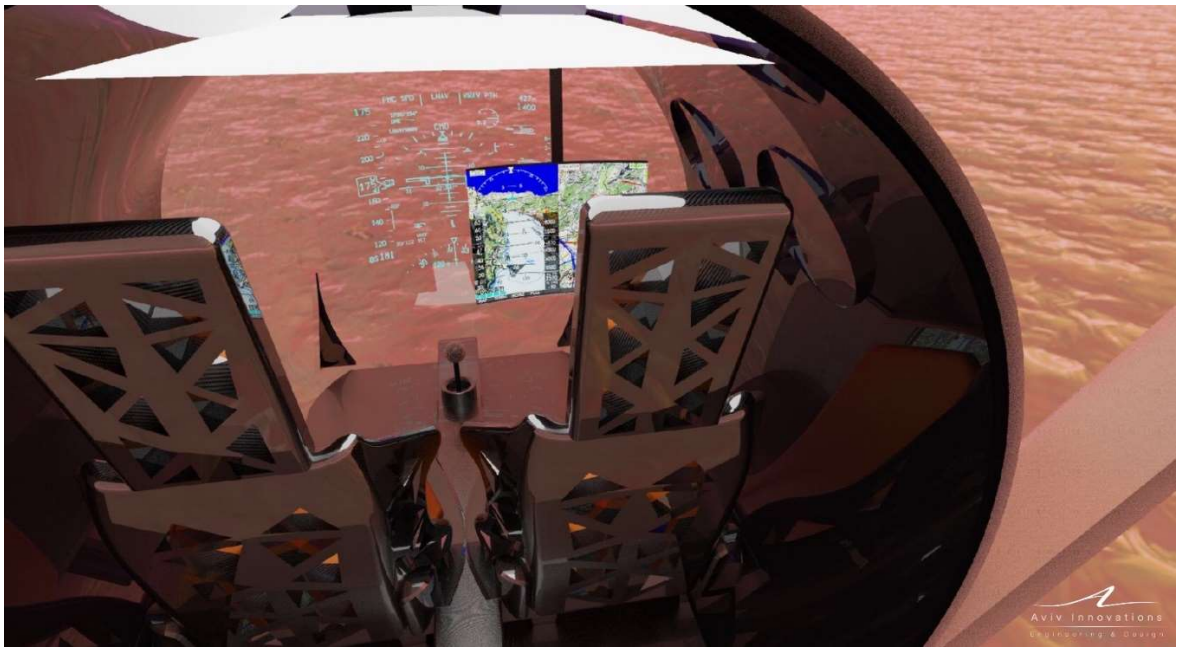

Figure 36 Cabin interior View

The structural analysis of the RMMP cabin and fuselage began with considerations of the interior cabin pressure which should be maintained. Hopefully, occupants will not have to wear full pressure suits, with the helmet on and locked, throughout the long flights. Presumably advanced space suits will be less bulky and stiff than current suits, perhaps relying upon elastic physical pressure rather than suit atmospheric pressure. With helmet removed and the elastic pressure relaxed, these would be like wearing long underwear. Still, there is a wide range of cabin pressurization values that could be assumed.

FAR 135.89 says pilots don't need oxygen up to 10,000 feet which gives 10.1 psi. That would be excellent if the weight penalty was not excessive. The upper limit of long-duration unpressurized cabins was probably defined by the B-17 which flew at 35,000 feet (3.5 psi). At that altitude an oxygen mask is required all the time, but otherwise it is acceptable provided that the cabin isn't too cold.

To investigate the weight penalty of different levels of pressurization and to validate the initial estimates of fuselage weight, trade studies were conducted using classical structural analysis equations. Benchmarks such as pressurized high-altitude earth-bound gliders and early manned spacecraft cabins were reviewed for comparison purposes.

The crew cabin is here analyzed as a composite overwrapped pressure vessel. It is divided into hemispherical, cylindrical and isotensoid segments. The shell weight and thickness for each segment is calculated individually. The highest thickness value obtained is then applied to all segments and the combined weight computed.

For hemispherical segment: thickness, $t_h = \dfrac{P * R}{2 * S * E - (0.2 * P)}$

weight, $w_h = (1.57) * \text{material density} * t_h * d_i^2$

For cylindrical segment: thickness, $t_c = \dfrac{P * R}{S * E - (0.6 * P)}$

weight, $w_c = \text{developed length} * \text{shell length} * \text{material density} * t_c$

where, developed length $= \pi (d_o - t_c)$

For torispherical segment: thickness, $t_t = \dfrac{(0.885) * P * L_i}{S * E - (0.1 * P)}$

weight, $w_t = \text{area} * \text{material density} * t_t$

where, area $= 1.084 * d_i^2$

where: P is Design Pressure, R is Inside Radius, S is Allowable Stress, E is Joint Efficiency; (E=1 here), d_i is Inside Diameter, d_o is Outside Diameter, L_i is Inside Length

This methodology was implemented in a spreadsheet program by Jaspreet Singh. For cabin internal operating pressures, a range of values corresponding to 10k, 21k and 35k feet in Earth atmosphere were evaluated as a trade study. Cabin shell thickness was sized to withstand a high bursting pressure (50 psi) based upon a maximum design value of 14.7 psi (Earth sea level). The overall weight estimated for the complete shell was in the range of 100 lbs. When insulation and secondary structure is accounted for with 25 mm wall thickness, the pressurized cabin structural weight is estimated around 390 lbs.

Based on this analysis the tentative decision is to pressurize to the equivalent of 10,000 ft., accepting a small weight penalty. This should be revisited in a detailed study, and may also be affected by the chosen pressurization level for the habitats on Mars.

XIII. Summary & Conclusions

Conceptual Research Corporation's Dr. Daniel P. Raymer, with the assistance of James French and an international team of volunteers, has completed the conceptual design of a manned utility aircraft to be operated by the permanent residents of Mars later this century. Nobody needs it now, and it assumes a level of human habitation on Mars that is only a dream at present, but that day will come.

The Raymer Manned Mars Plane is designed for exploration, research, cargo transport, photography, and the linking of multiple settlements. Its minimum required capabilities are equivalent to the original Army Jeep, namely a crew of two plus cargo to a total of 500 lbs, carried at least 260 nmi. Its flight control system allows fully autonomous flight for cargo transport and extraction missions, with VTOL operation.

The design study results suggest that such a manned Mars airplane is possible, with the application of advanced but feasible technologies in the post-2030 time frame. The RMMP-2 configuration shown above is a viable option but just the first in a long process of trade study and optimization to converge to a best solution.

Sincere thanks go to contributors/co-authors James French, Felix Finger, Arturo Gómez, Jaspreet Singh, Ramlingam Gyanasampath Pillai, Matheus Monjon, Joabe Marcos de Souza, and Aviv Levy.

Special thanks to Robert Zubrin, author of the influential book *The Case for Mars*[2], for his original Haiku written for this paper. In a personal email Zubrin also offers the possibility of relaxing an onerous design requirement assumed above, commenting "I agree that the lack of paved runways on Mars is deplorable. I will see what I can do about correcting it."

References

[1] Young, L., Pisanich, G., Ippolito, C., "Aerial Explorers," AIAA Aerospace Sciences Meeting, Reno, NV, 2005

[2] Zubrin, R., *The Case For Mars*, Touchstone/Simon & Schuster, New York, NY, 1996

[3] anon., "Vehicle Profiles: Jeep Willys," The Classic Cars Journal (https://journal.classiccars.com), 2 July 2008

[4] Raymer, D., *Living In The Future: The Education and Adventures of an Advanced Aircraft Designer*, Design Dimension Press, Los Angeles, CA, 2009

[5] Adams, D., *Life, the Universe and Everything*, Pan Books, London, 1982

[6] French, J., "Rocket Propellants from Martian Resources," Journal of the British Interplanetary Society Vol 42, 1989

[7] Raymer, D., "RDSwin: Seamlessly-Integrated Aircraft Conceptual Design for Students & Professionals", AIAA Paper 2016-1277, AIAA Aerospace Sciences Meeting, San Diego, CA, 2016

[8] Raymer, D., *Aircraft Design: A Conceptual Approach,* American Institute of Aeronautics and Astronautics, Washington, D.C., 1989 (6th Edition 2018)

[9] Raymer, D., *Simplified Aircraft Design for Homebuilders*, Design Dimension Press, Los Angeles, CA, 2003

[10] F. Götten, D. F. Finger, M. Marino, C. Bil, M. Havermann and C. Braun, "A Review of Guidelines and Best Practices for Subsonic Aerodynamic Simulations using RANS CFD," Asia-Pacific International Symposium on Aerospace Technology - APSIAT 2019, Gold Coast, Australia, 2019

[11] Tilley, Alvin R. *The Measure of Man and Woman: Human Factors in Design,* Wiley, NY, NY, 2001